Instabilities and Plasma Heating in the Inner Heliosphere: Thermodynamics far from Equilibrium

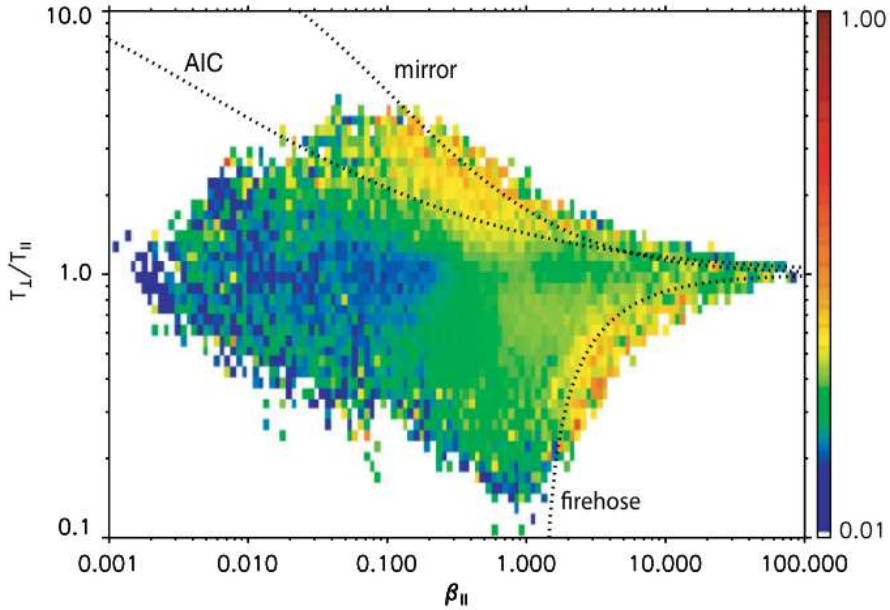

Bale et al 2009 Wind

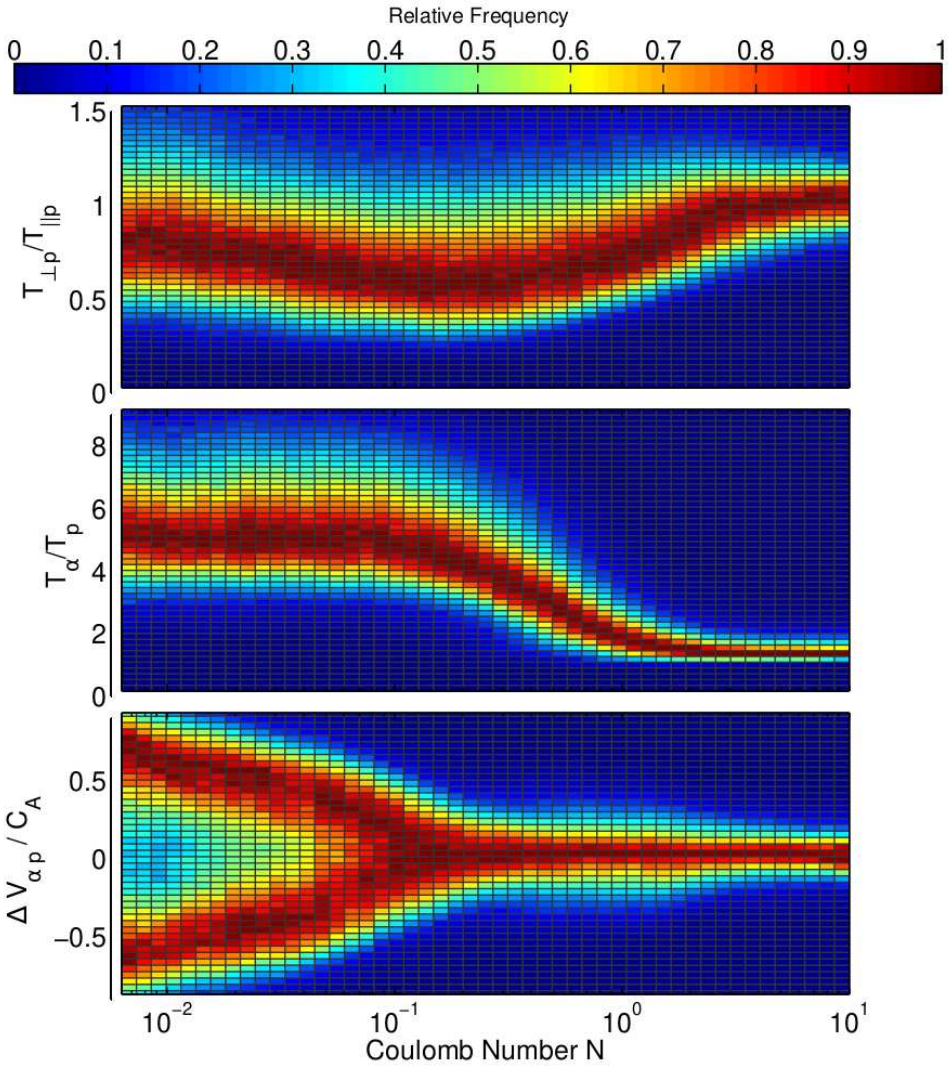

Kasper et al 2017 Wind

Kristopher G. Klein (U. Arizona)

PPPL Heliophysics Seminar

28 Mar, 2019

THE UNIVERSITY OF ARIZONA
COLLEGE OF SCIENCE
LUNAR & PLANETARY LABORATORY

In Collaboration With:

Justin Kasper, Benjamin Alterman, Daniel Vech (U. Michigan)
Mike Stevens, Kelly Korreck (Harvard Smithsonian)
Daniel Verscharen (University College London)

With funding support from grants
NASA HSR NNX16AM23G and NNX16AG81G

The Solar Wind Frequently Departures from LTE

Particle Velocity Distributions $f_s(\mathbf{v})$

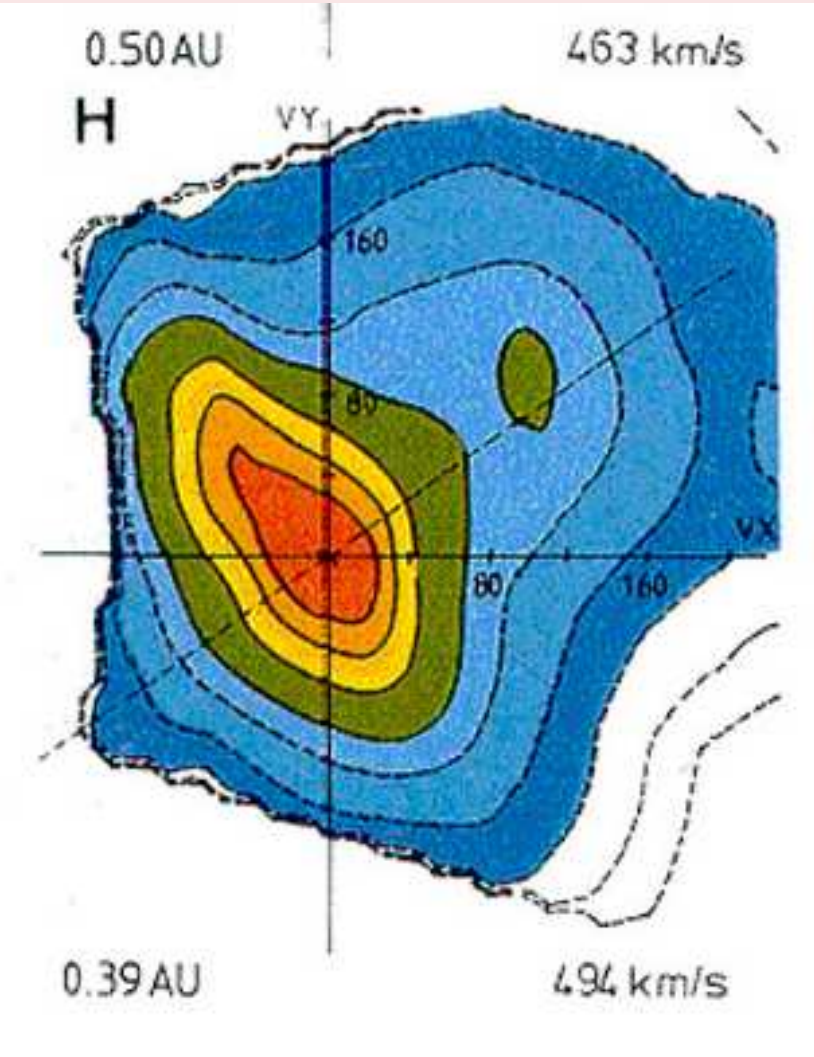

Marsch et al, 2012: Helios

Due to its hot, diffuse nature, collisions are unable to enforce a Maxwellian distribution in the solar wind:

$$\nu_{a,b} \approx 4\pi \frac{q_a^2 q_b^2 n_b \ln \Lambda}{m_a^2 w_b^3} \propto nT^{-3/2}$$

Typical structures include:

- $T_\perp \neq T_\parallel$
- $T_i \neq T_j$
- relative drifts
- agyrotropy

'Collisionality' Organizes Non-Equilibrium Structure

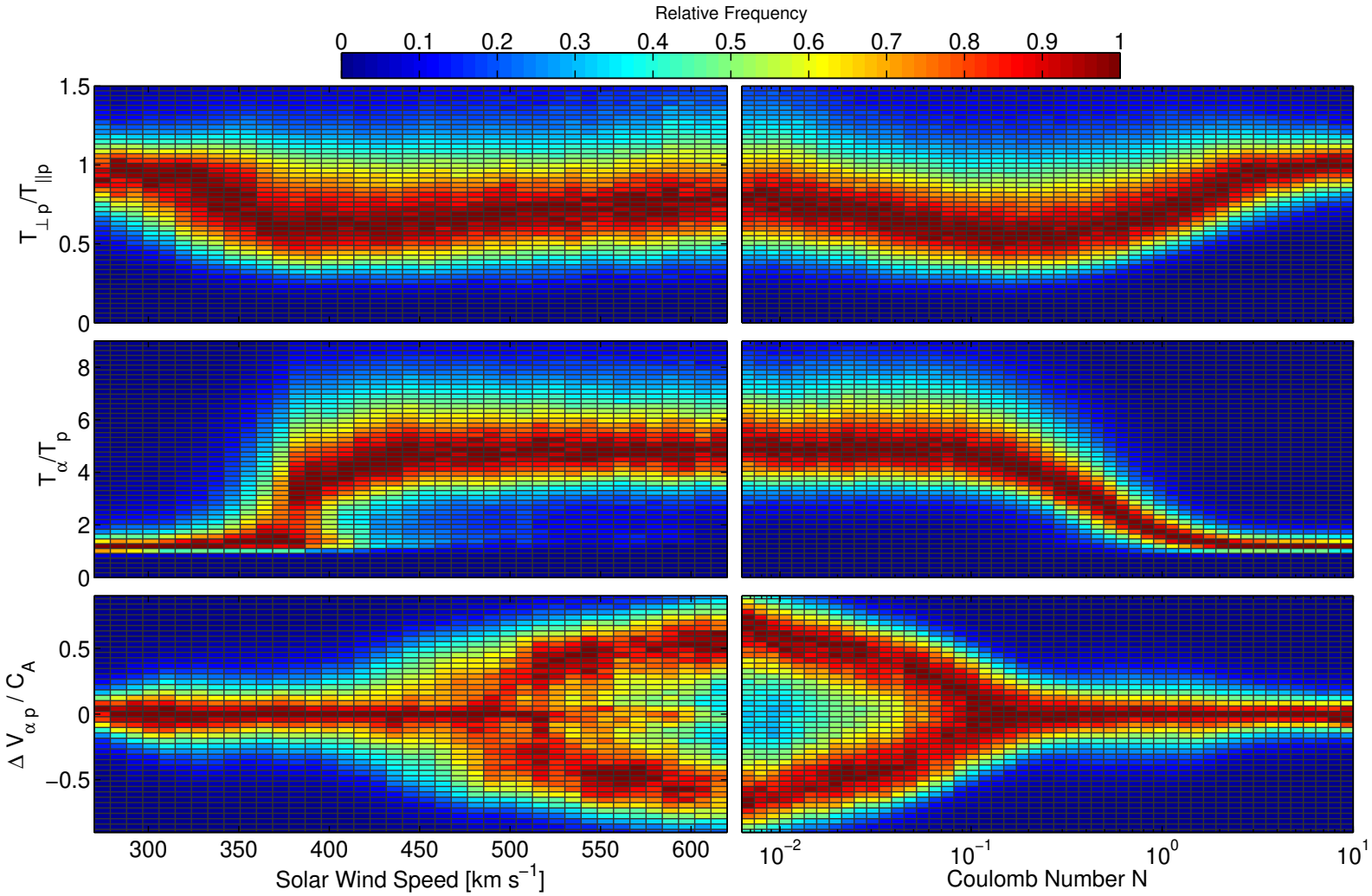

Kasper et al, 2017: Wind

$$N_c = \nu_{a,b}\frac{R}{V_{sw}}$$

How Can We Use Departures from Equilibrium to Understand the Solar Wind?

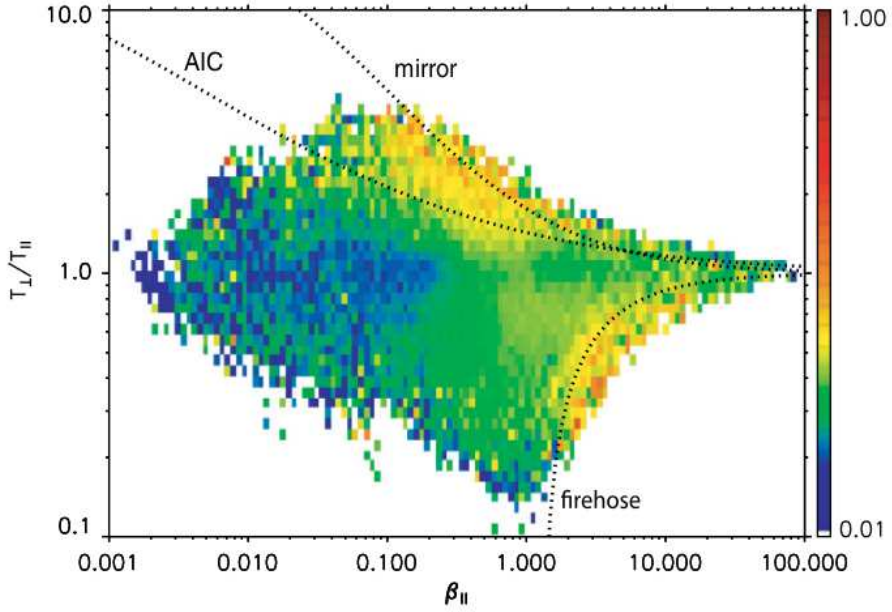

Bale et al 2009 Wind

- As Driver of Dynamics
- As Diagnostic of Remote Processes

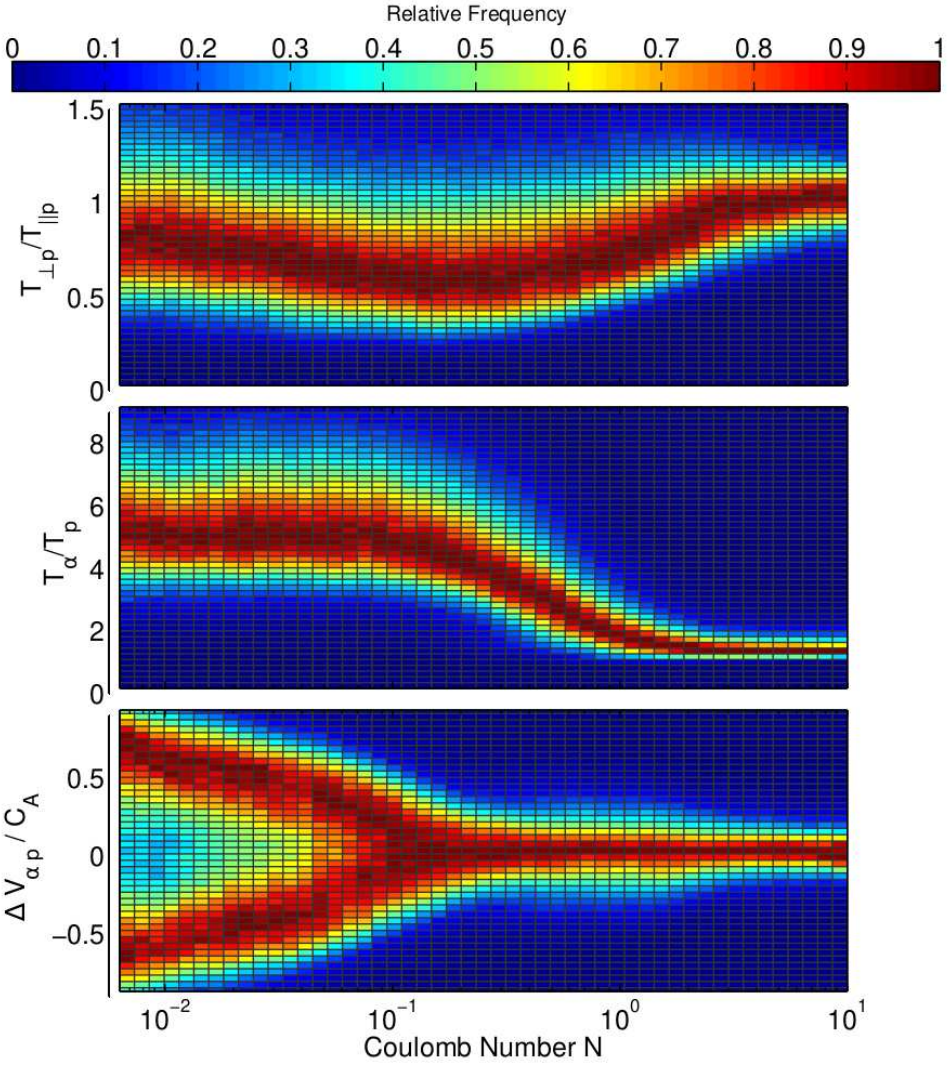

Kasper et al 2017 Wind

Extracting Energy from non-Maxwellian Distributions

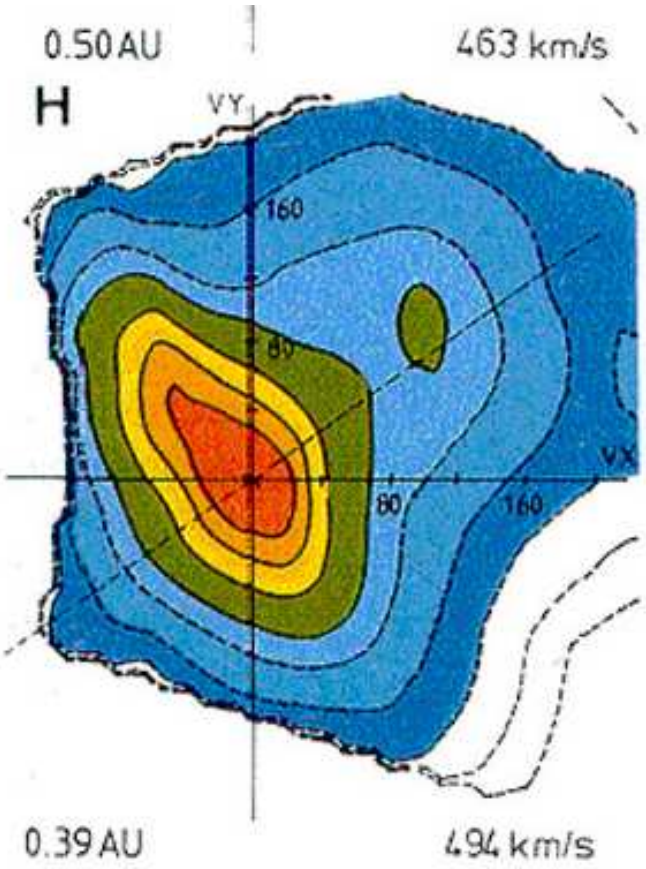

Marsch 2012 Helios

For this work, we focus only on linear stability.

Fluid Firehose Instability:

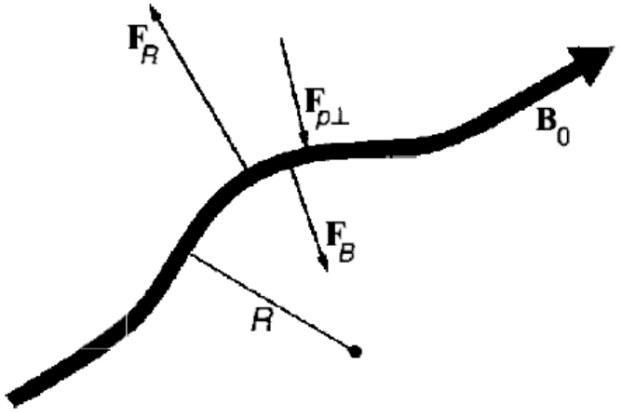

Treumann & Baumjohann, 1997

Cyclotron **Resonant** Instability:

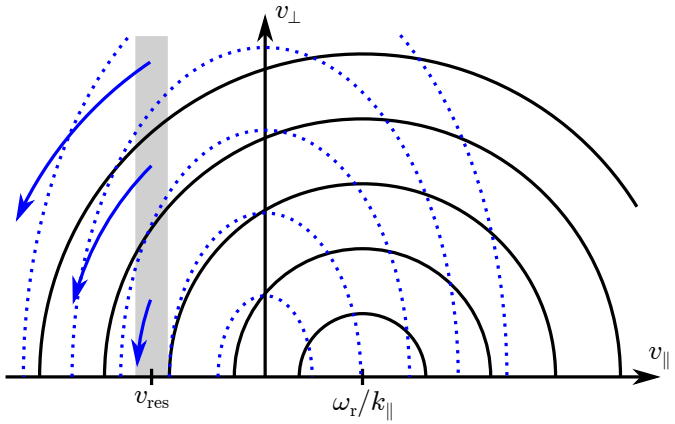

Verscharen, Klein, & Maruca, under review

Simple Models for Stability Thresholds

Focusing on a single free-energy source and assuming an analytic form for $f_p(v_\perp, v_\parallel)$, we parameterize where specific instabilities arise.

$$\frac{T_{\perp,p}}{T_{\parallel,p}} = 1 + \frac{a}{\left(\beta_{\parallel,p} - \beta_0\right)^b}$$

Hellinger et al. 2006

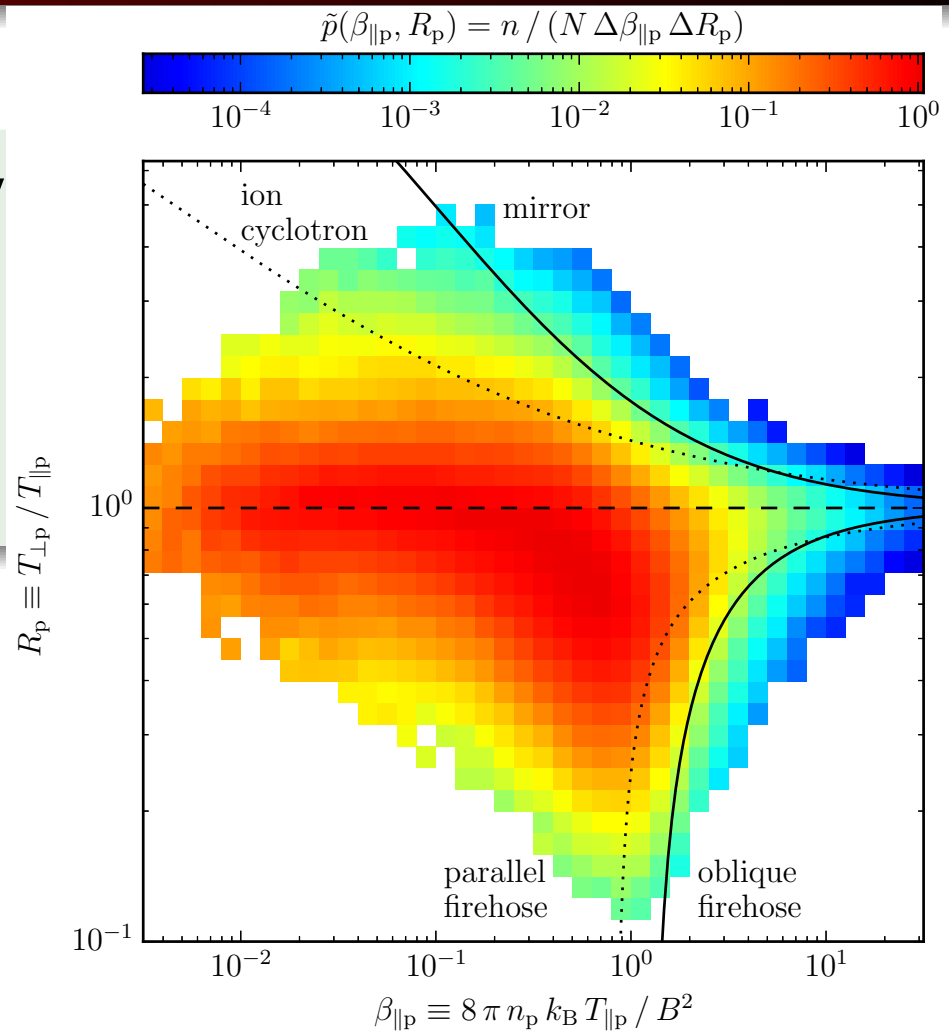

Verscharen, Klein, & Maruca, under review Wind

Such models do not account for other energy sources (e.g. other species anisotropies, relatively drifting components)

Instabilities Limit the Solar Wind's Evolution

Matteini et al 2007

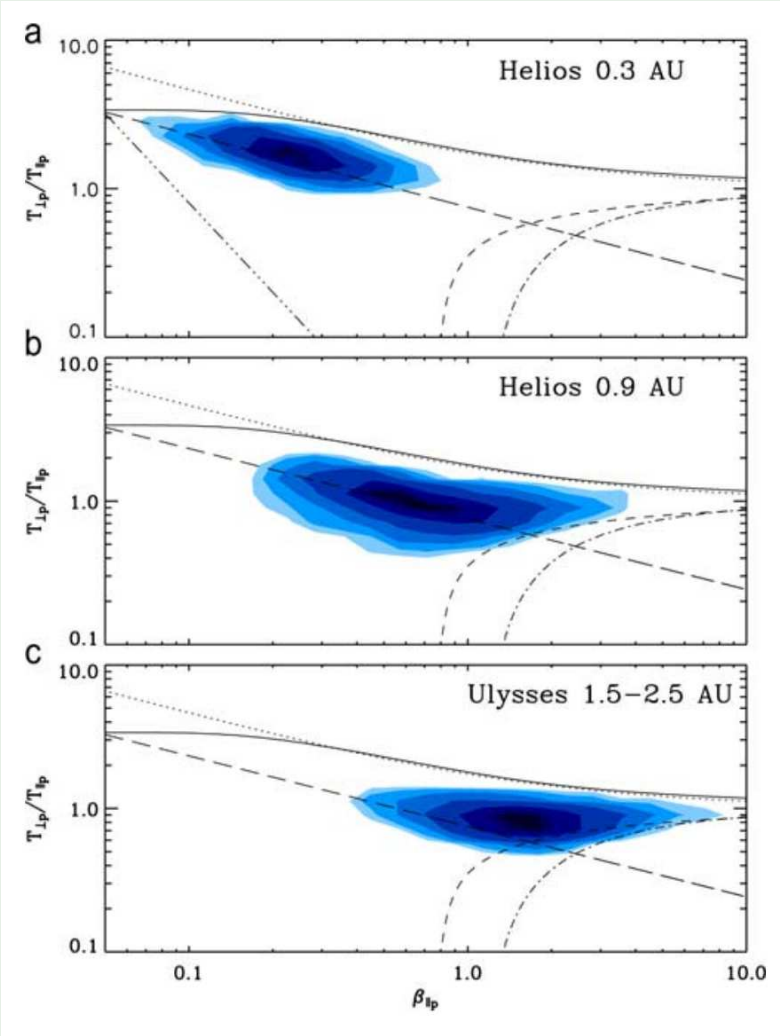

Bale et al 2009

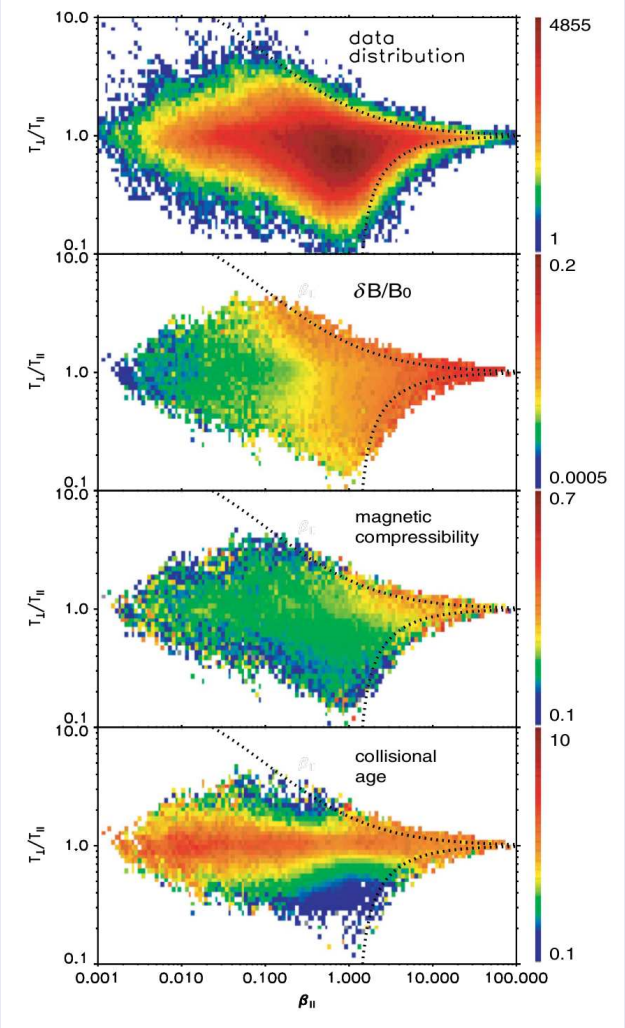

These correlations may mask underlying dependencies.

(Hellinger & Travnicek 2014)

Advanced Models for Stability Thresholds

$$\Lambda_{\text{firehose}} = \frac{\beta_{\parallel} - \beta_{\perp}}{2} + \frac{\sum_s \rho_s |\Delta \mathbf{v}_s|^2}{\rho v_A^2} > 1$$

$$\Lambda_{\text{mirror}} = \sum_s \beta_{\perp s} \left(\frac{\beta_{\perp s}}{\beta_{\parallel s}} - 1 \right) + \frac{\left(\sum_s q_s n_s \frac{\beta_{\perp s}}{\beta_{\parallel s}} \right)^2}{2 \sum_s \frac{(q_s n_s)^2}{\beta_{\parallel s}}} > 1$$

Kunz et al 2015

These models only account for configuration-space instabilities, and in the case of Λ_{mirror} neglects drifts.

A study of resonant instabilities will require other tools.

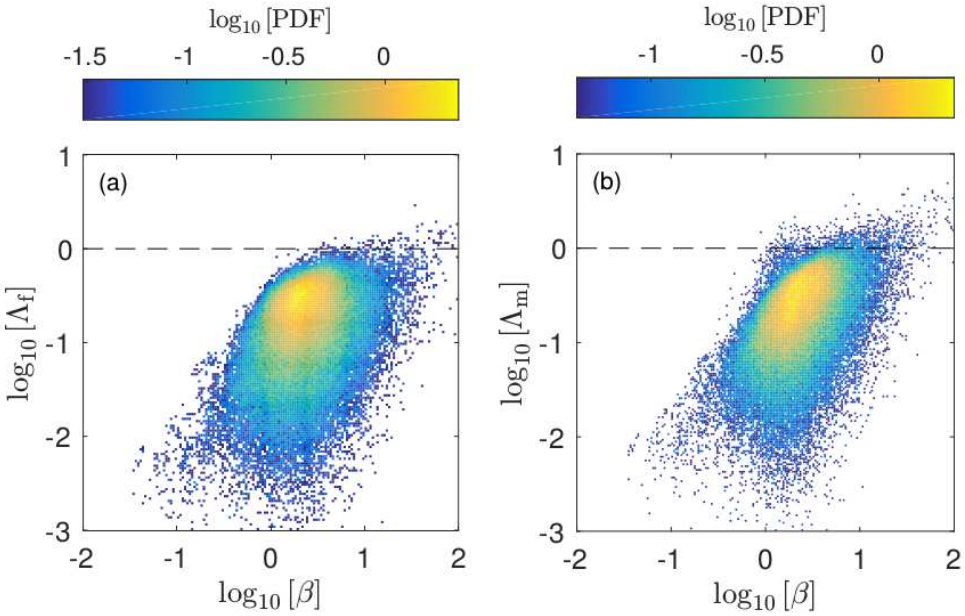

Chen et al 2016 Wind

Identifying Instabilities from Linear Dispersion Relation $|\mathcal{D}|$

Given the wave vector equation

$$\mathbf{n} \times (\mathbf{n} \times \mathbf{E}) + \underline{\underline{\epsilon}} \cdot \mathbf{E} = \underline{\underline{\mathcal{D}}} \cdot \mathbf{E} = 0$$

normal modes (ω, γ) arise for $|\mathcal{D}| = 0$.

We model $|\mathcal{D}|$ for the solar wind using:

- a collection of N_s bi-Maxwellian distributions
- drifting relative to one another
- with a background magnetic field

Normal modes are a function of $6N_s - 1$ parameters:

- wavevector $k_\perp \rho_R, k_\parallel \rho_R$
- 'global' plasma parameters $\beta_{\parallel,R}$ and $v_{t,\parallel,R}/c$
- the ratios $T_\perp/T_\parallel|s$, $T_{\parallel,R}/T_{\parallel,s}$, n_s/n_R, m_s/m_R, q_s/q_R, and $V_{\mathrm{drift},\parallel,s}/v_{AR}$ for each population s

Identifying Instabilities from Linear Dispersion Relation $|\mathcal{D}|$

Given the wave vector equation

$$\mathbf{n} \times (\mathbf{n} \times \mathbf{E}) + \underline{\epsilon} \cdot \mathbf{E} = \underline{\underline{\mathcal{D}}} \cdot \mathbf{E} = 0$$

unstable modes are solutions $|\mathcal{D}| = 0$ in complex frequency space (ω, γ) that have a positive damping rate $\gamma > 0$.

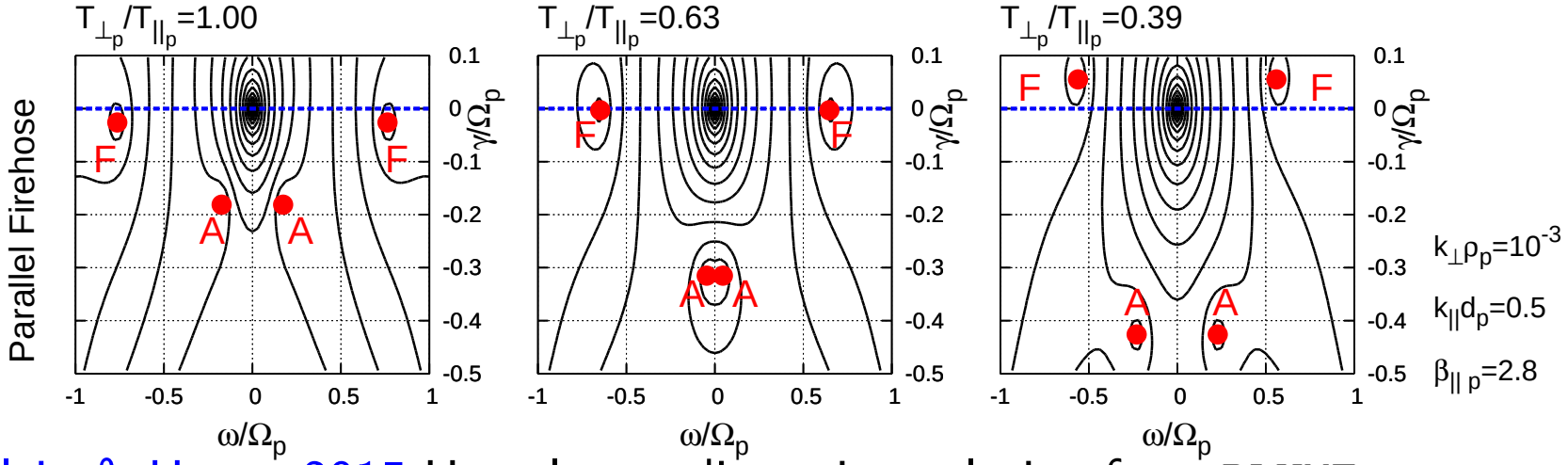

Klein & Howes 2015 Hot plasma dispersion solution from PLUME

Stability sensitively depends on the bulk parameters of each species, which cover a wide range of values in the solar wind, making implementing a manual scan time consuming.

The Nyquist Instability Criterion (Nyquist 1932, Penrose 1960)

Instead of searching for solutions of $|D(\omega,\gamma)| = 0$ with $\gamma > 0$, we evaluate the contour integral for the number of unstable modes:

$$W_n = \frac{1}{2\pi i} \oint \frac{d\omega}{|D(\omega,\gamma)|}.$$

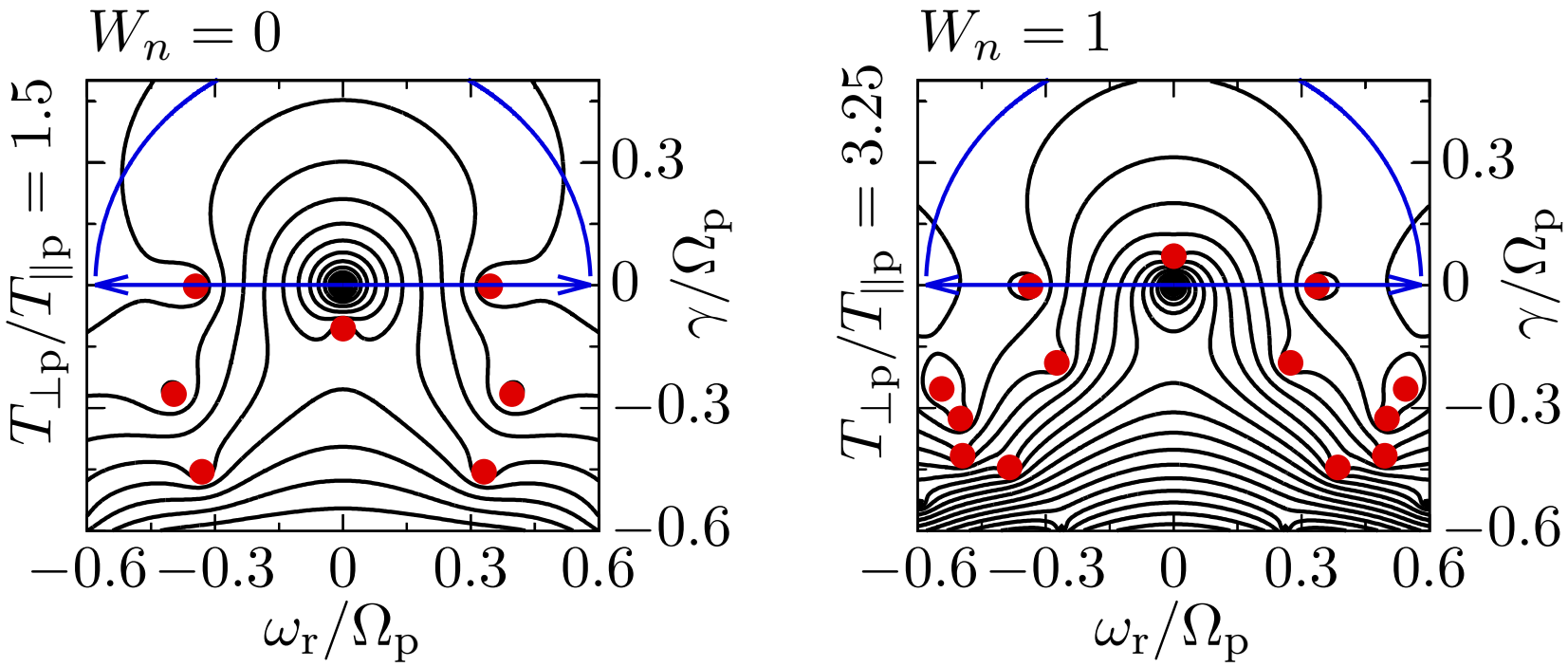

We have numerically implemented a winding number calculator using the PLUME dispersion solver (Klein et al. 2017 JGR).

We can test for arbitrarily fast growing modes

Instead of using $\gamma = 0$ to define the contour,
we calculate W_n for any growth rate γ_{min}

(This requires the insertion of a branch cut).

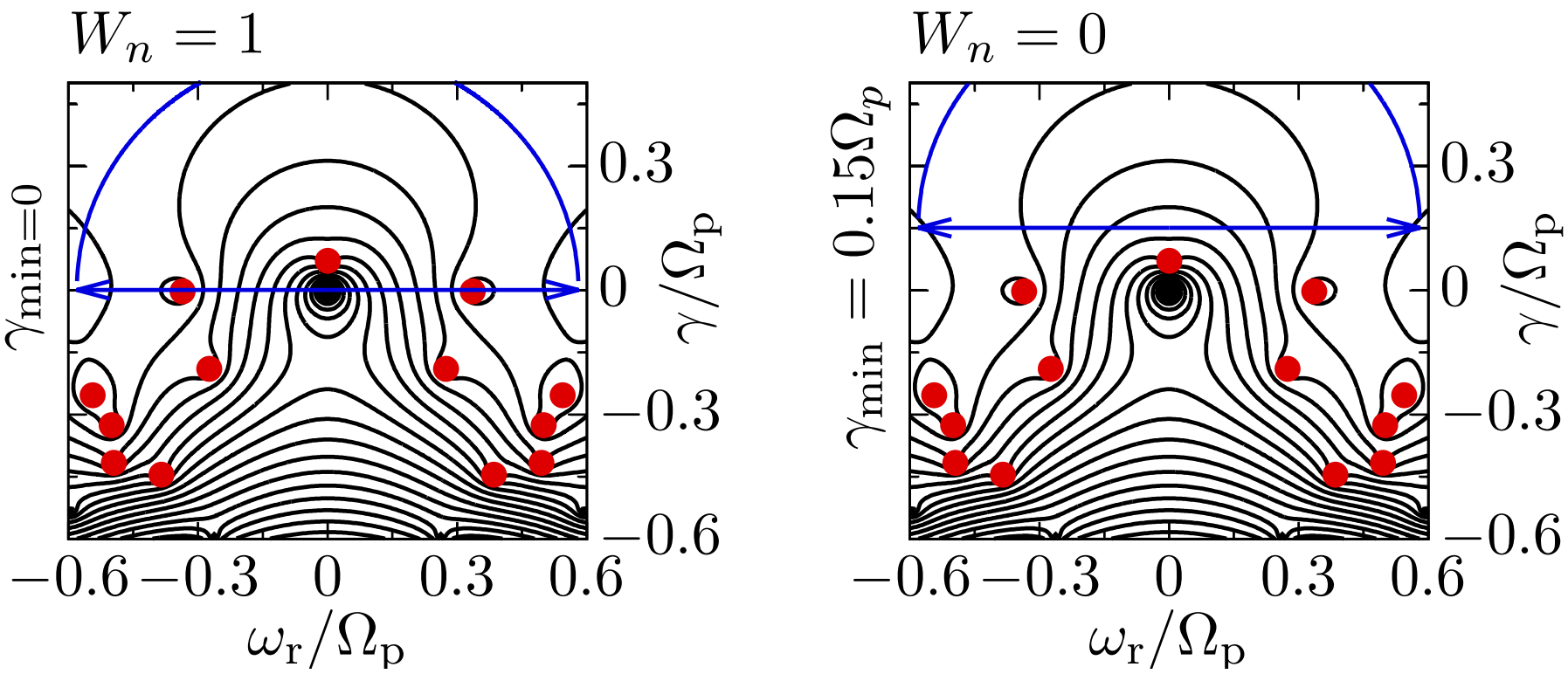

Modes with $\gamma < \gamma_{\mathrm{min}}$ will not be included in the calculation.

A Solar Wind Relevant Example

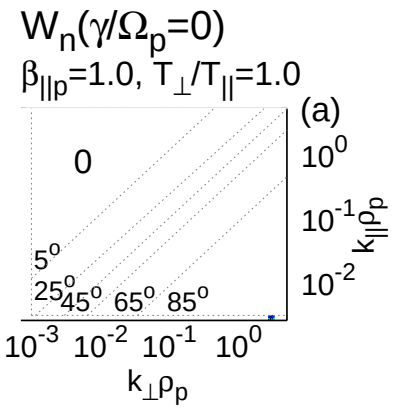

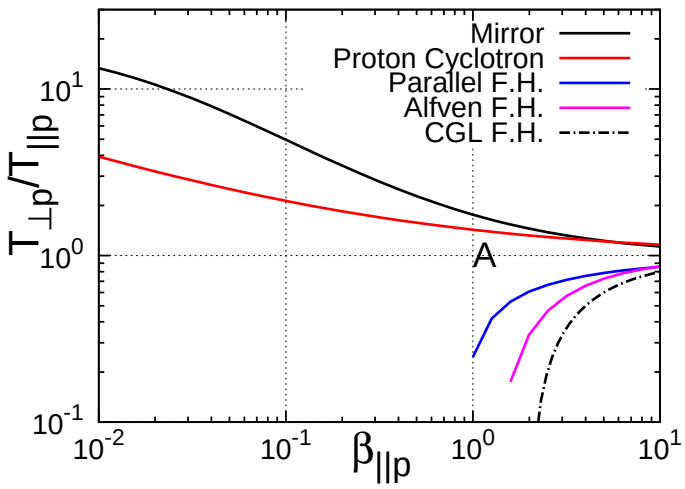

To Verify Our Algorithm

we calculate $W_n(\mathbf{k})$ for points in the $(\beta_{||p}, T_{\perp p}/T_{||p})$ plane using PLUME's hot, magnetized plasma dispersion relation.

A Solar Wind Relevant Example

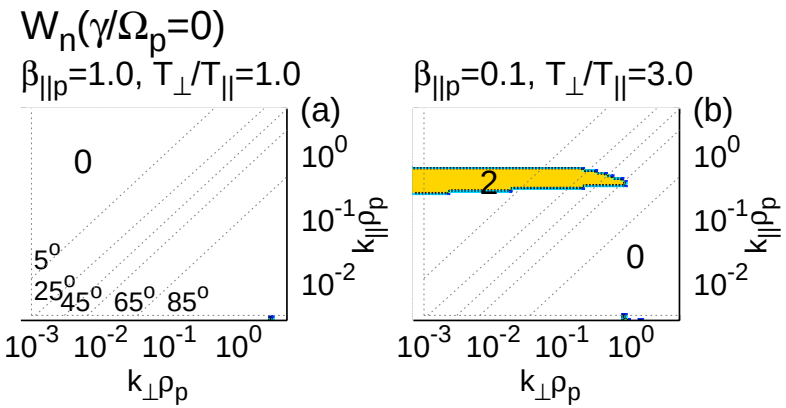

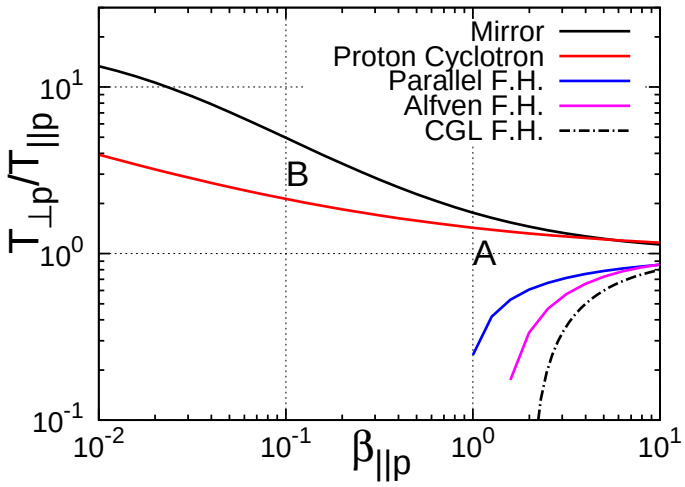

To Verify Our Algorithm

we calculate $W_n(\mathbf{k})$ for points in the $(\beta_{||p}, T_{\perp p}/T_{||p})$ plane using PLUME's hot, magnetized plasma dispersion relation.

A Solar Wind Relevant Example

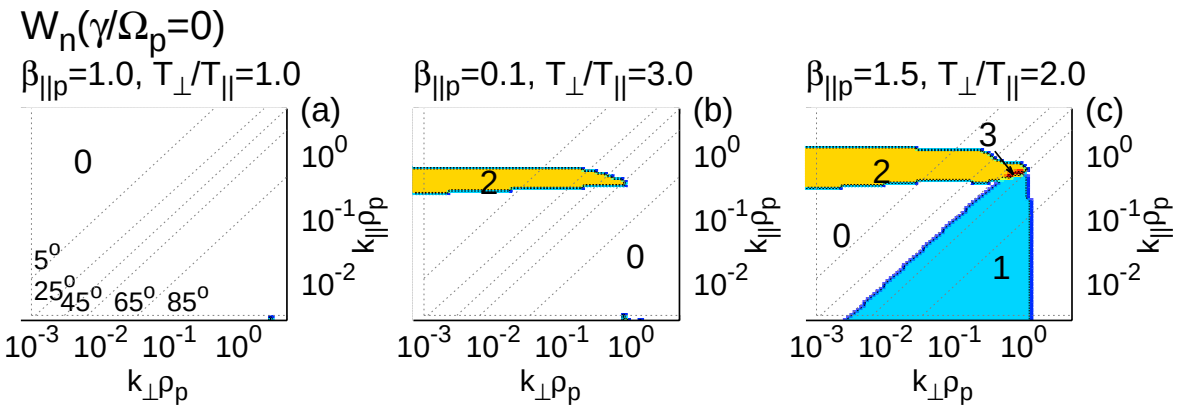

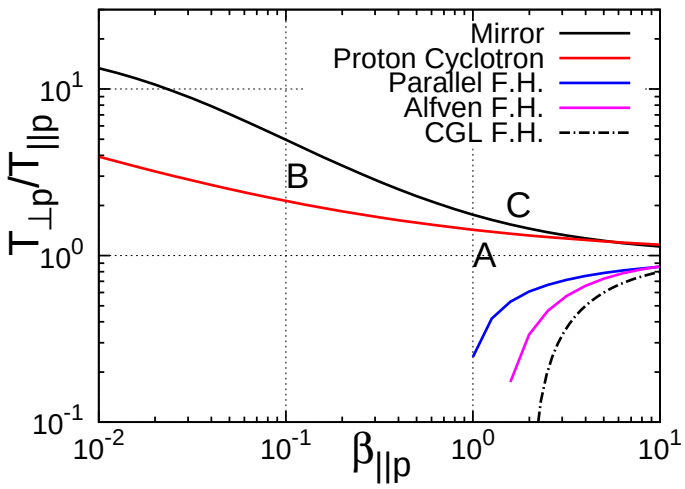

To Verify Our Algorithm

we calculate $W_n(\mathbf{k})$ for points in the $(\beta_{||p}, T_{\perp p}/T_{||p})$ plane using PLUME's hot, magnetized plasma dispersion relation.

A Solar Wind Relevant Example

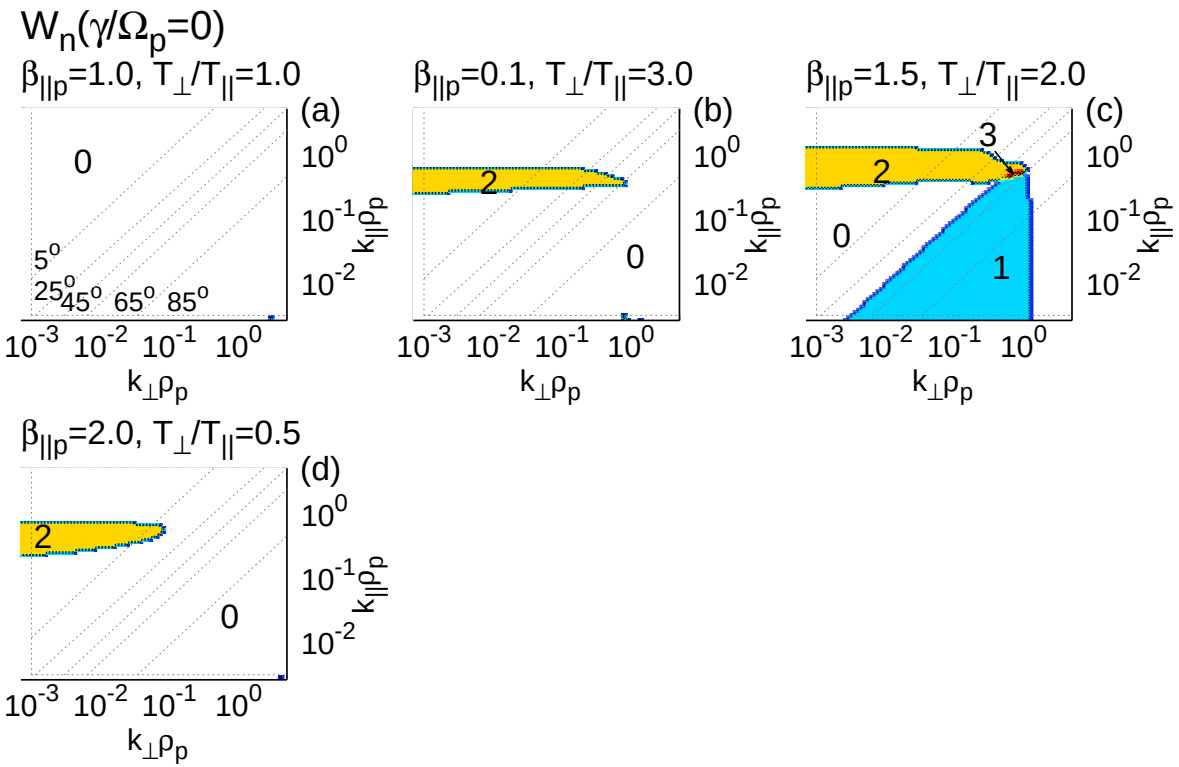

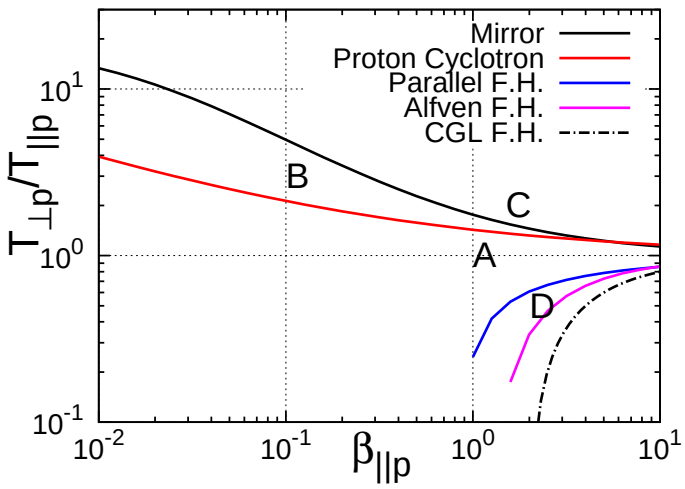

To Verify Our Algorithm

we calculate $W_n(\mathbf{k})$ for points in the $(\beta_{||p}, T_{\perp p}/T_{||p})$ plane using PLUME's hot, magnetized plasma dispersion relation.

A Solar Wind Relevant Example

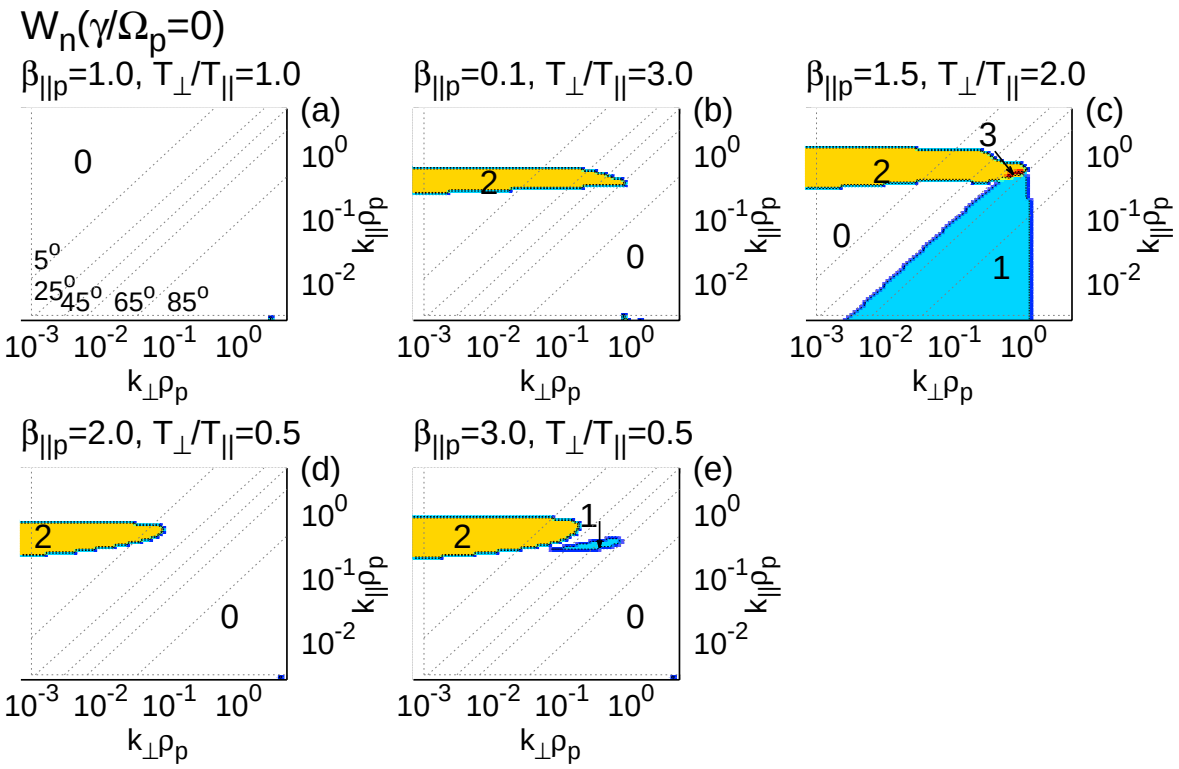

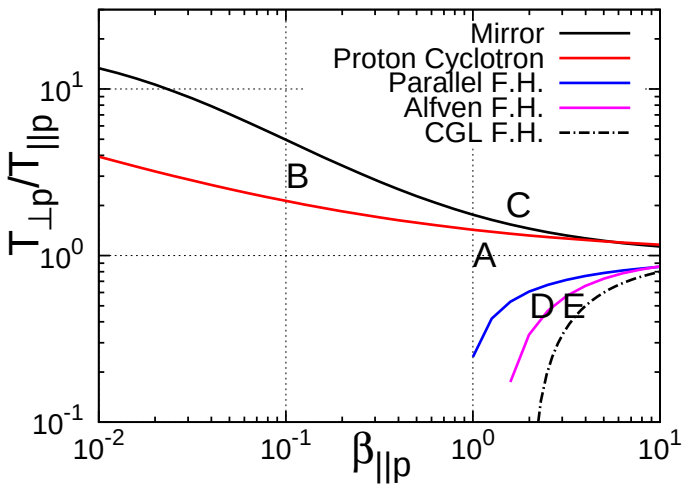

To Verify Our Algorithm

we calculate $W_n(\mathbf{k})$ for points in the $(\beta_{||p}, T_{\perp p}/T_{||p})$ plane using PLUME's hot, magnetized plasma dispersion relation.

A Solar Wind Relevant Example

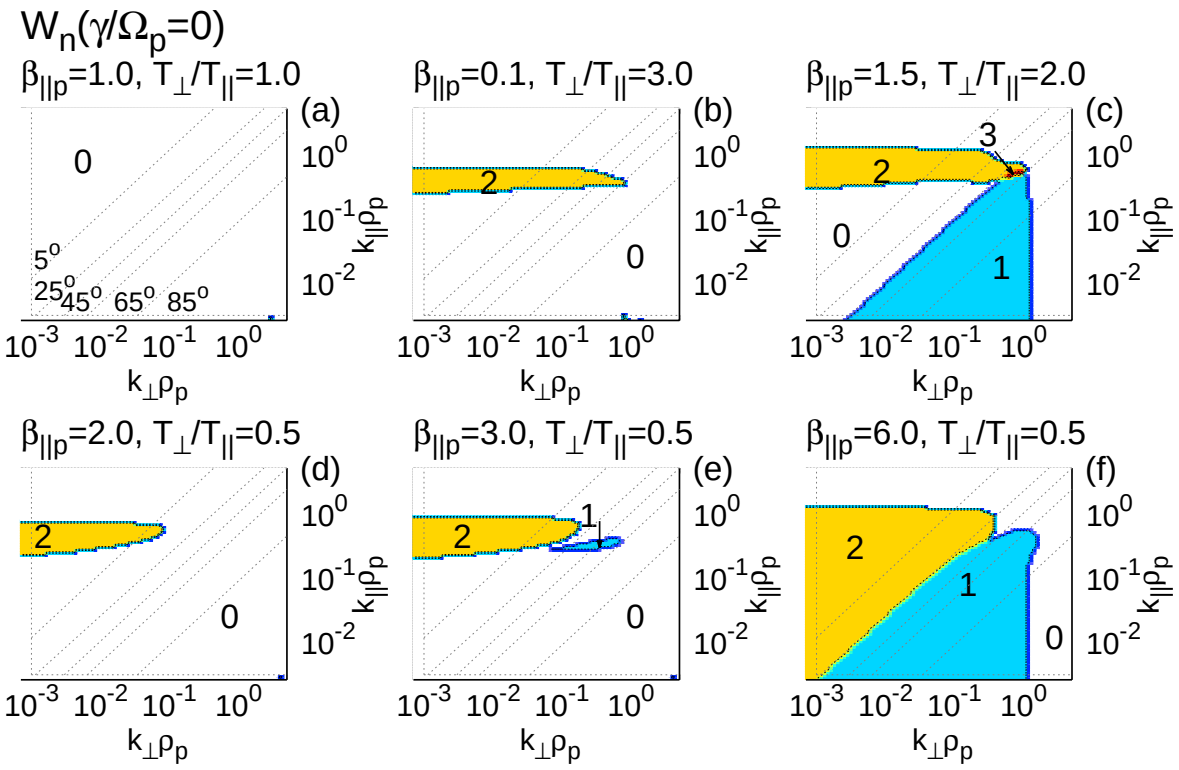

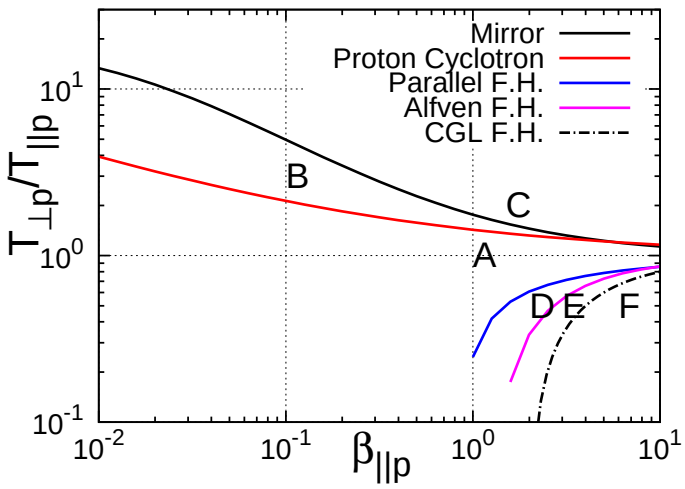

To Verify Our Algorithm

we calculate $W_n(\mathbf{k})$ for points in the $(\beta_{||p}, T_{\perp p}/T_{||p})$ plane using PLUME's hot, magnetized plasma dispersion relation.

Faster Growing Modes

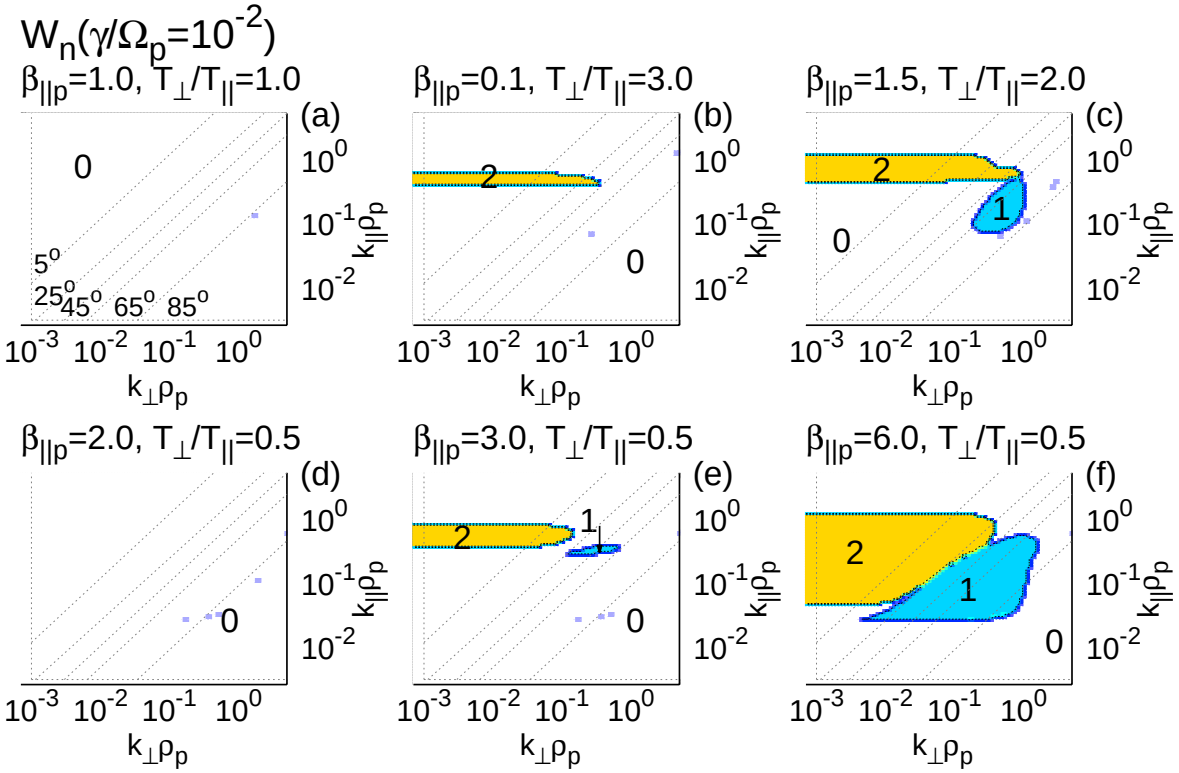

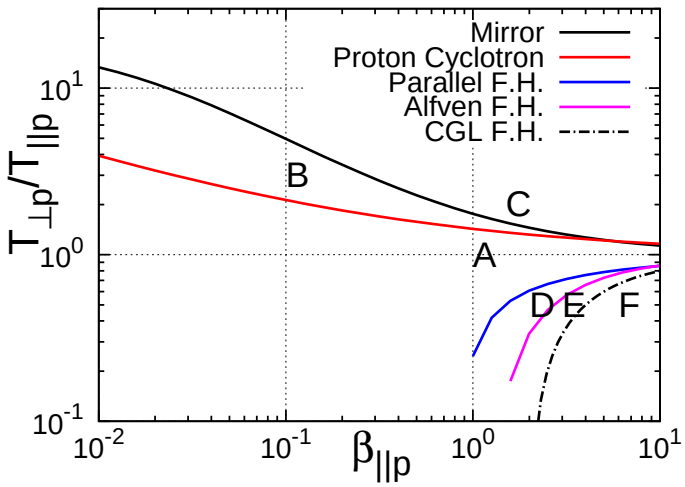

Instead of using the $\gamma = 0$ contour,
we calculate W_n for $\gamma_{\min} = 10^{-2}\Omega_p$.

Comparisons to Actual Solar Wind Measurements

Gary et al 2016; Wind

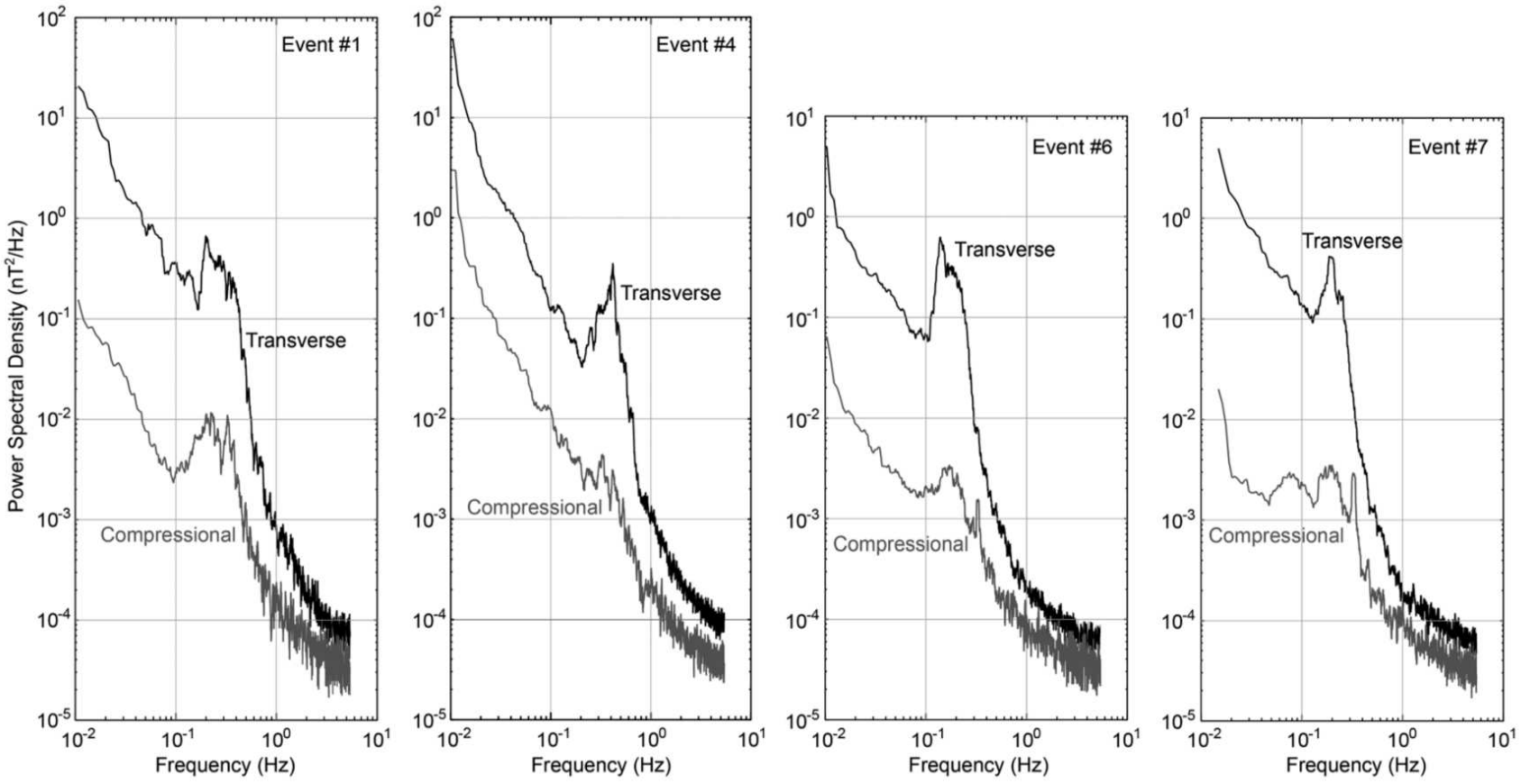

Identified 6 intervals with observational signatures of parallel propagating instabilities in the magnetic power spectra.

Which Modes are Driven Unstable?

Using drifting, bi-Maxwellian moments for the proton core & beam, He^{++}, and e^{-}

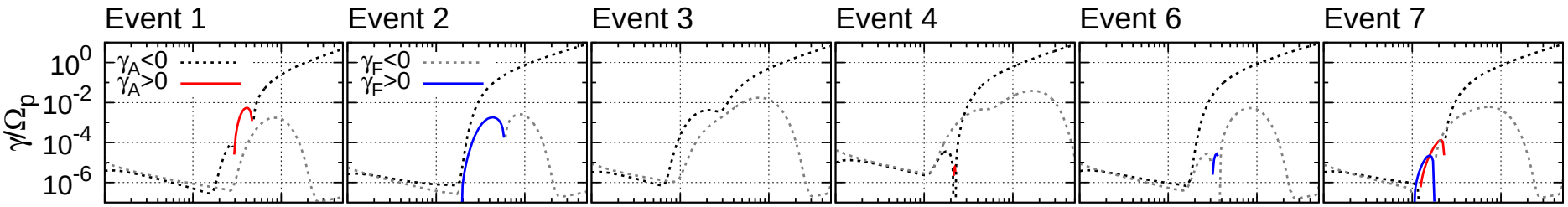

Klein et al 2017

Only two events have modes with growth rates $\gamma > 10^{-3}\Omega_p$.

How Does Our Analysis Compare?

Using drifting, bi-Maxwellian moments for the proton core & beam, He^{++}, and e^{-}

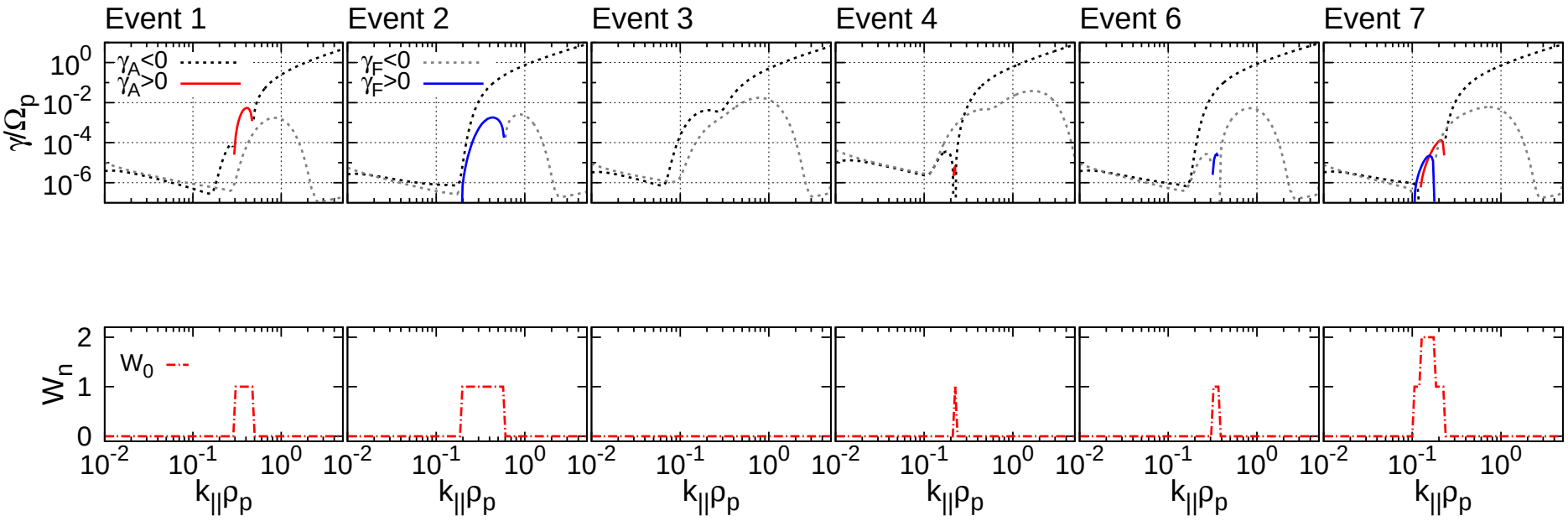

Klein et al 2017

Our W_n calculation agrees with the normal mode analysis.

How Robust are these Results?

10 % Monte Carlo variation of
proton core & beam, He^{++}, and e^{-} parameters.

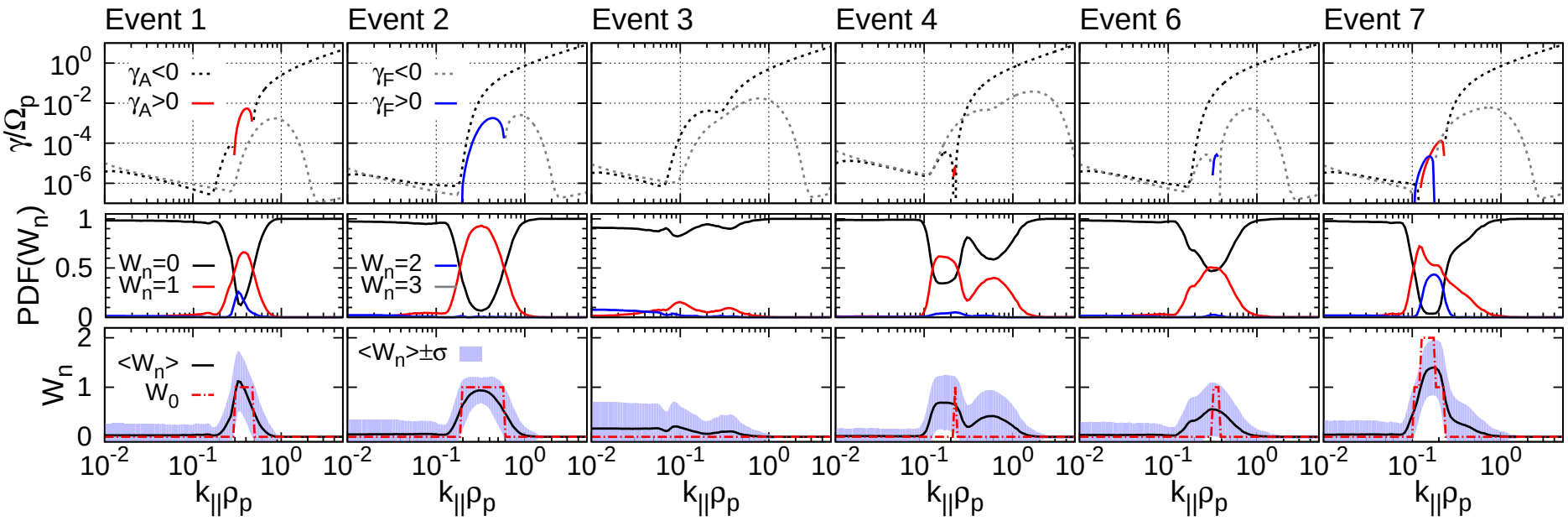

Klein et al 2017

Events 4 & 6 are near unstable regions of parameter space

A Statistical Data Set from the Solar Wind

- We select a random set of Wind spectra, the first nominal spectra a day from 309 days in 2016 & 2017.
- For each spectrum, a nonlinear-least-squares Bi-Maxwellian fit is performed for up to three ion components;
  proton core $n_p, T_{\perp p}, T_{\| p}$,
  proton beam $n_b, T_{\perp b}, T_{\| b}, \Delta v_{pb}$,
  α **population** $n_\alpha, T_{\perp \alpha}, T_{\| \alpha}, \Delta v_{p\alpha}$,
  and combined with $|B|$ to produce the associated dimensionless parameters. (Klein et al 2018)

- For Each Spectra, we calculate $W_n(\mathbf{k}\rho_p)$ on a grid covering $(k_\perp, k_\|)\rho_p \in [10^{-2}, 10^1]$.
- The maximum growth rates of unstable spectra are found within $\gamma_{\min}/\Omega_p = [10^{-4}, 1]$.

Occurrence of Ion-Driven Instabilities

	# Spectra	# Unstable	Mirror	CGL FH	Kinetic
Total	309	166	14	1	151
p, b, & α	189	130	12	0	118
p & α	114	33	2	1	30
p & b	5	3	0	0	3
p	1	0	0	0	0

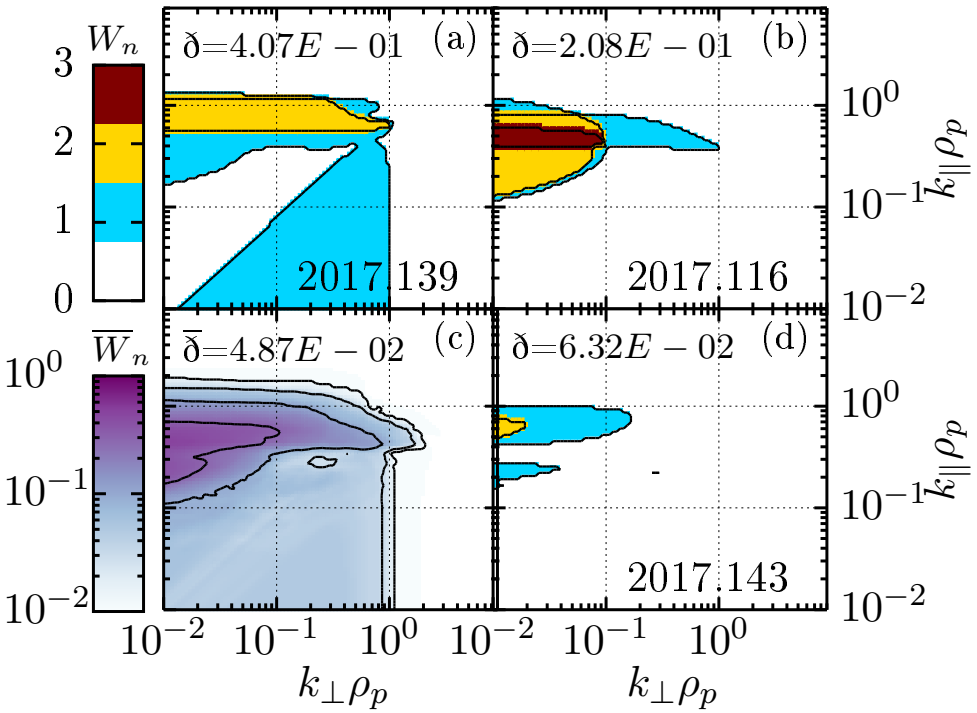

- 54% of spectra are unstable
- The majority of the instabilities are kinetic, i.e. $k_\perp \rho_p < k_\parallel \rho_p \lesssim 1$
- Instabilities preferentially arise when a proton beam is resolved

Klein et al 2018

No Instabilities Have Growth Rates Exceeding Ω_p^{-1}

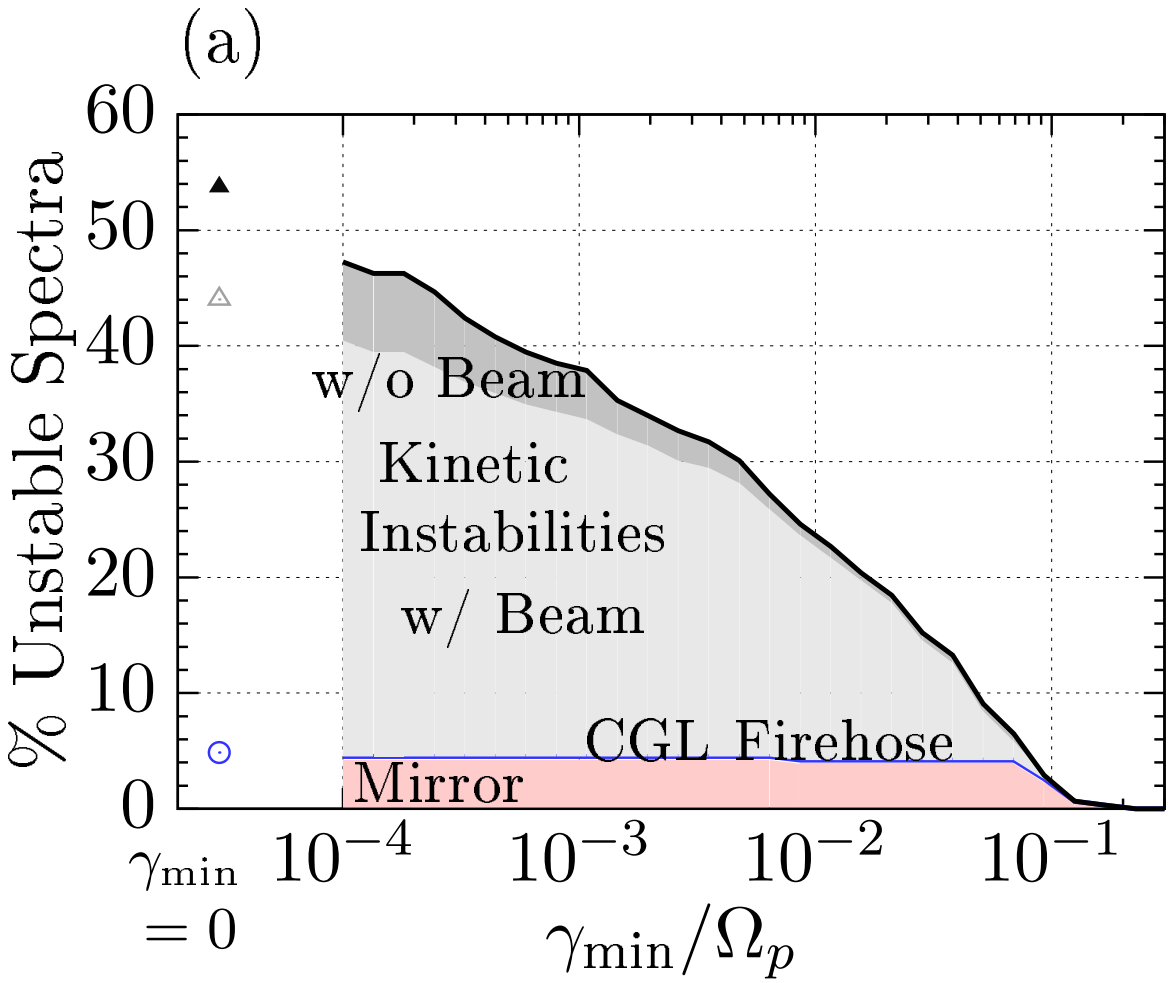

- Recalculating W_n for increasing $\gamma_{\min}$ shows all observed instabilities have $\gamma \lesssim 0.1\Omega_p$
- The fluid instabilities have the largest growth rates, while unstable intervals w/o proton beams are generally less virulent

Klein et al 2018

Comparison to Other Timescales

We re-scale the stability fraction as a function of alternative timescales:

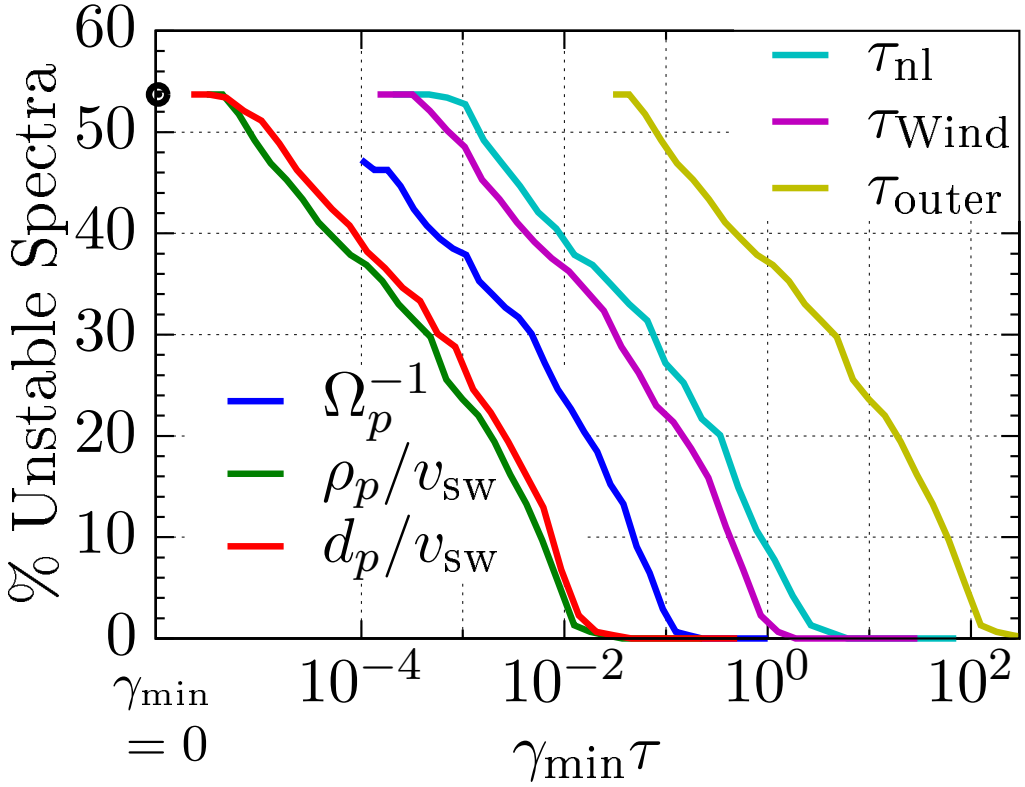

- $\frac{\rho_p}{v_{\rm sw}} = \frac{w_{\perp,p}}{\Omega_p v_{\rm sw}}$
- $\frac{d_p}{v_{\rm sw}} = \frac{v_A}{\Omega_p v_{\rm sw}}$
- $\tau_{\rm Wind} = 92{\rm s}$
- $\tau_{\rm nl} = (k_0\rho_p)^{1/3}\frac{\rho_p}{v_A}$
- $\tau_{\rm outer} = \frac{L_0}{v_{\rm sw}} = \frac{2\pi}{k_0 v_{\rm sw}}$

- The ion-kinetic timescales and $\tau_{\rm Wind}$ are faster than γ
- 10% of the spectra have γ comparable to the cascade time at $k_\perp\rho_p = 1$.

Comparing To Temperature Anisotropy Thresholds

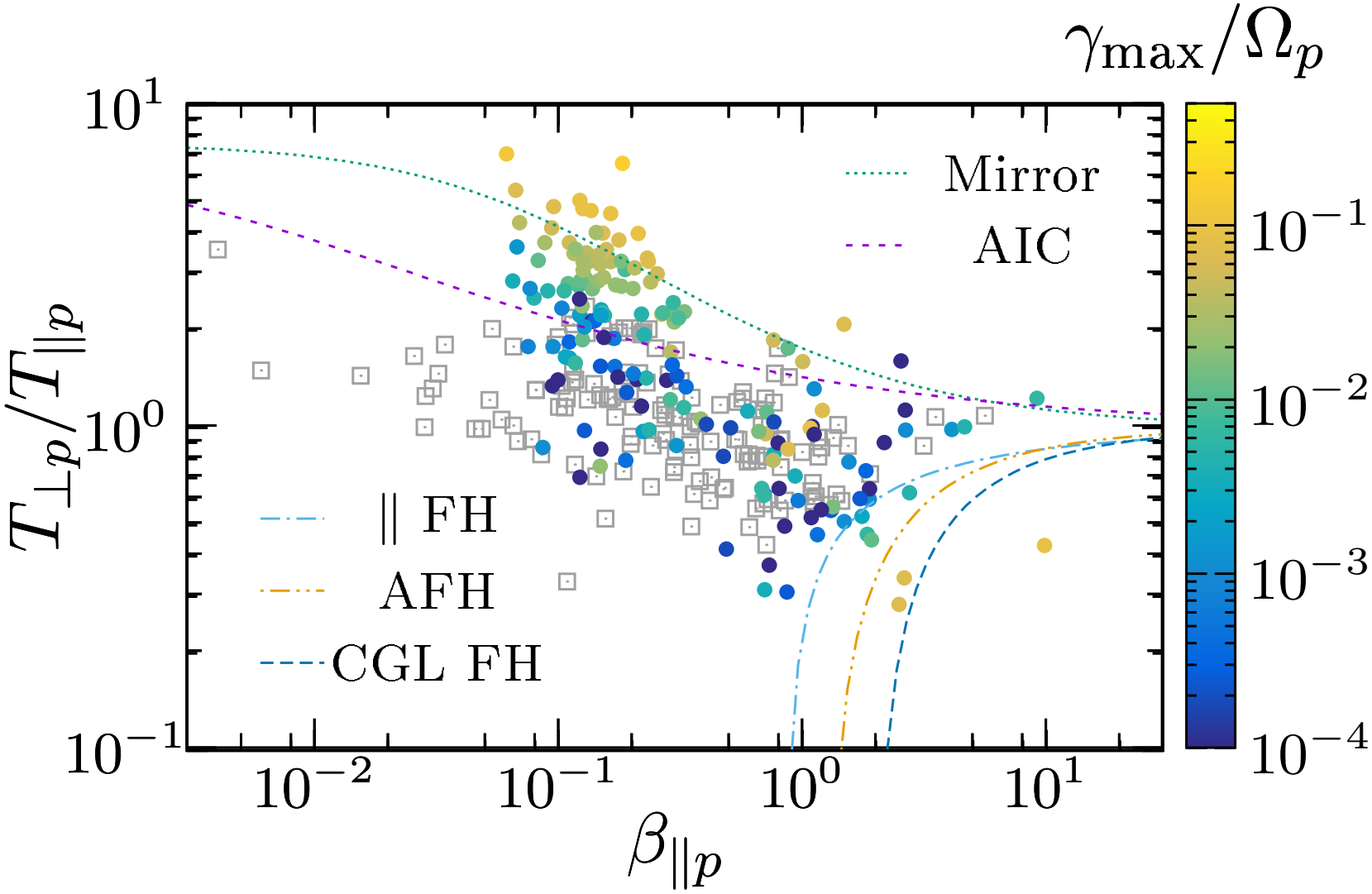

A significant fraction of spectra in the 'stable' region support growing modes. (Klein et al 2018)

ALPS: Extending beyond bi-Maxwellians

Arbitrary **L**inear **P**lasma **S**olver (`ALPS`, Verscharen et al 2018, JPP) solves the full hot-plasma dispersion relation for a set of plasma populations with **arbitrary** velocity distributions defined on a grid in momentum space.

We are applying our instability algorithm to solar wind distributions using `ALPS`, identifying configurations where the bi-Maxwellian and actual stability differ.

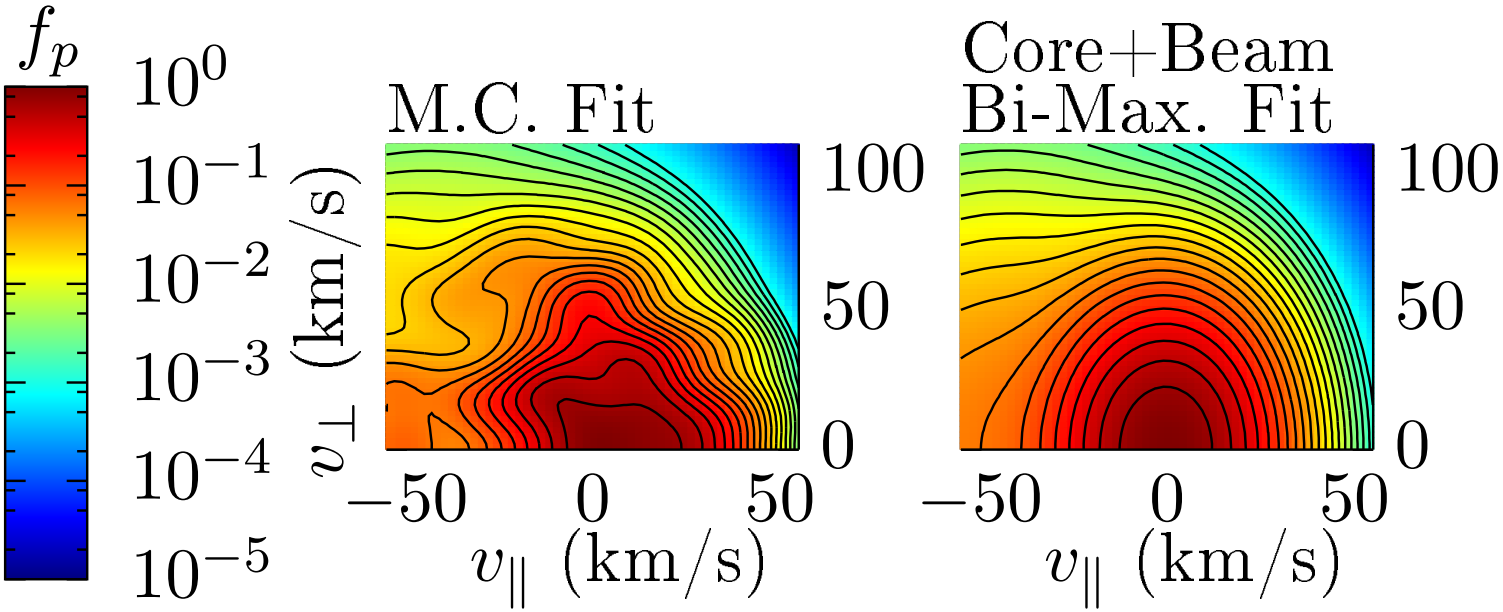

Diagnosing Remote Plasma Processes

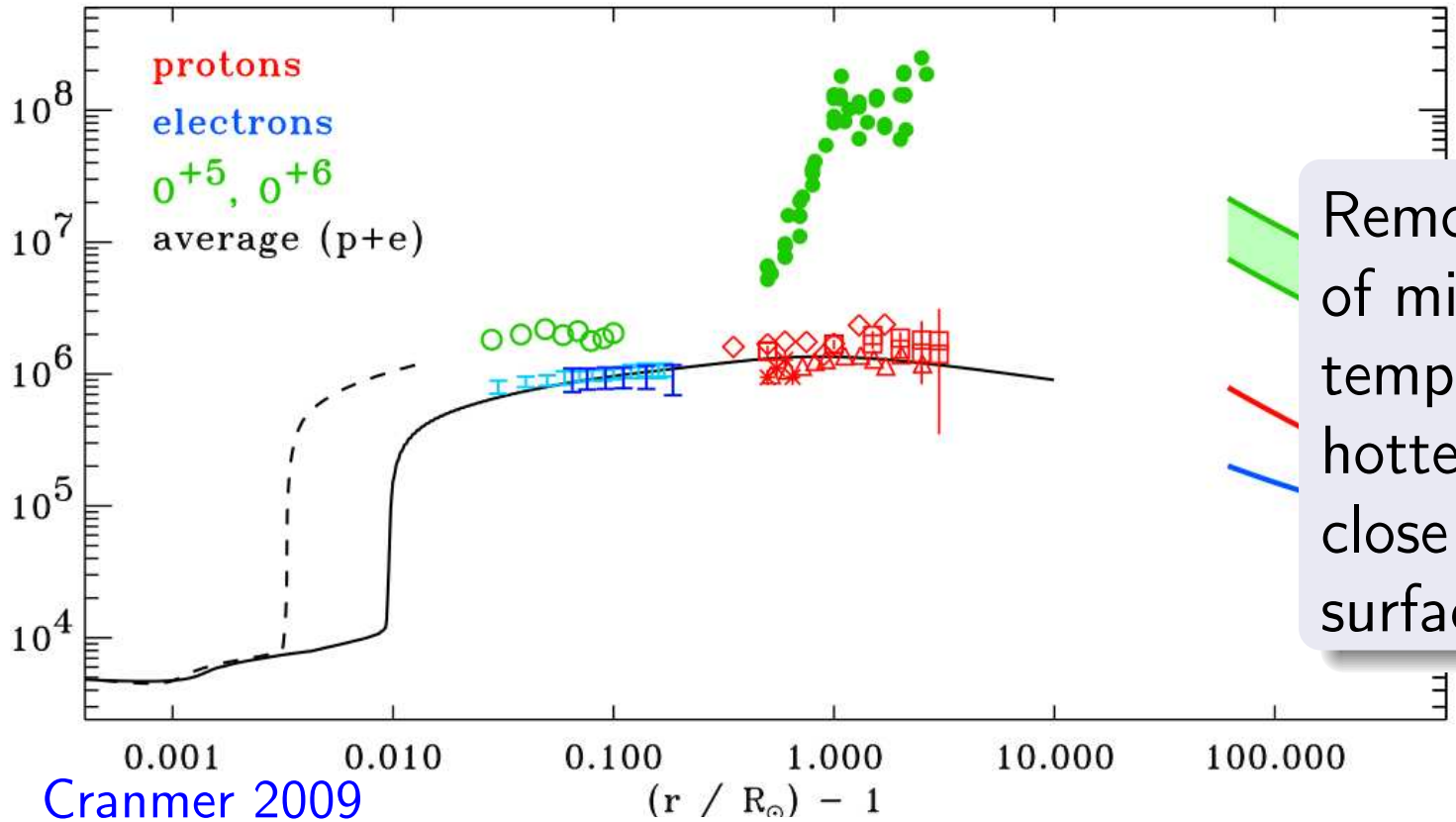

Cranmer 2009

Remote observations of minor ions indicate temperatures 10x hotter than protons close to the Sun's surface

What Mechanisms Act to Preferentially Heat Minor Ions?
And Where Do They Operate?

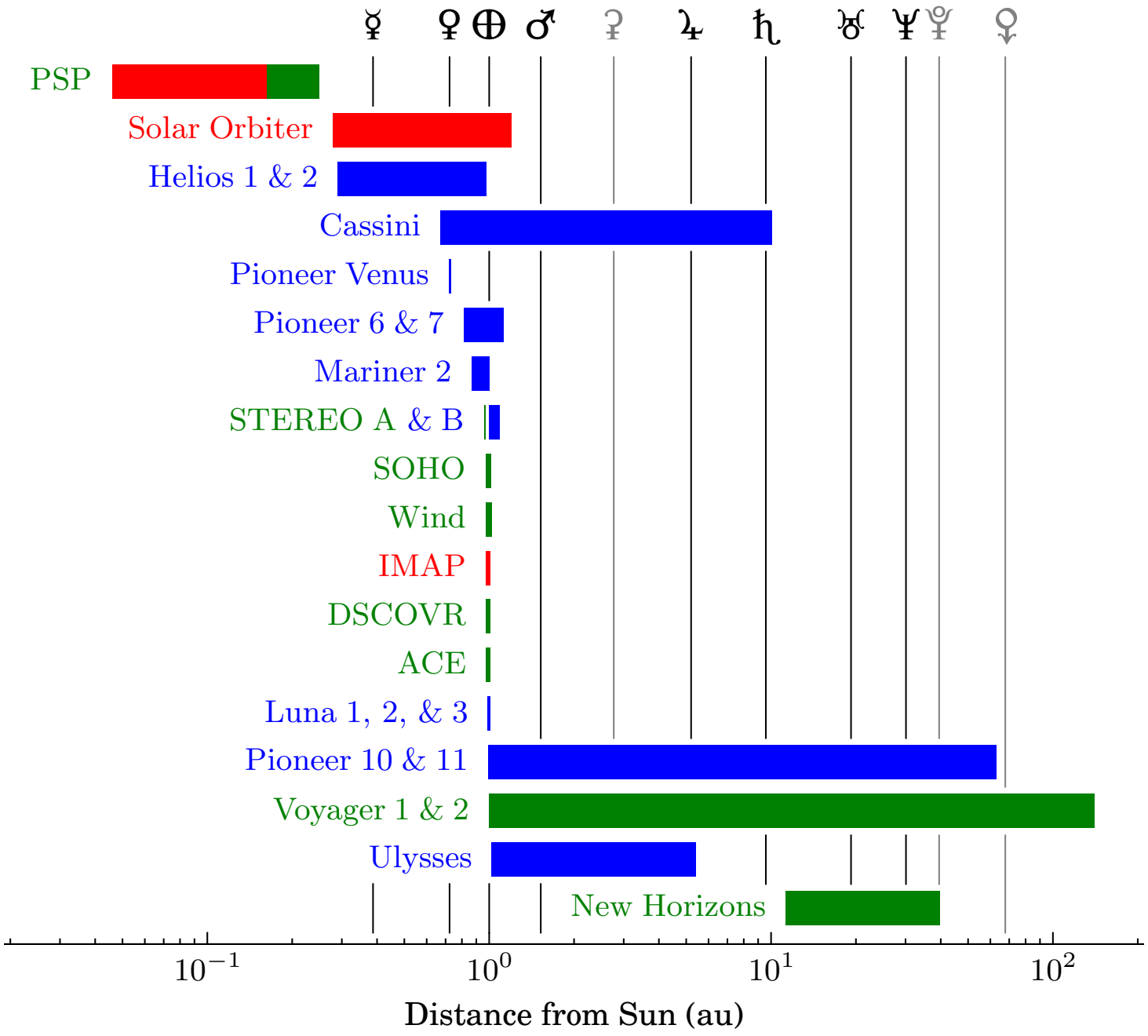

Verscharen, Klein, & Maruca, under review

$T_\alpha/T_p(N_c)$ Suggests Collisional Thermalization

Considering the evolution of temperature differences in the absence of any effects other than Coulomb collisions, keeping T_p constant, and following Spitzer (1962), we can write

$$\frac{d(T_\alpha/T_p)}{dt} = -\nu_{\alpha,p}\frac{T_\alpha}{T_p}$$

$$\rightarrow$$

$$\frac{T_\alpha}{T_p} \sim \exp\left[-\int \nu_{\alpha,p}dt\right]$$

$$\sim \exp\left[-N_c\right]$$

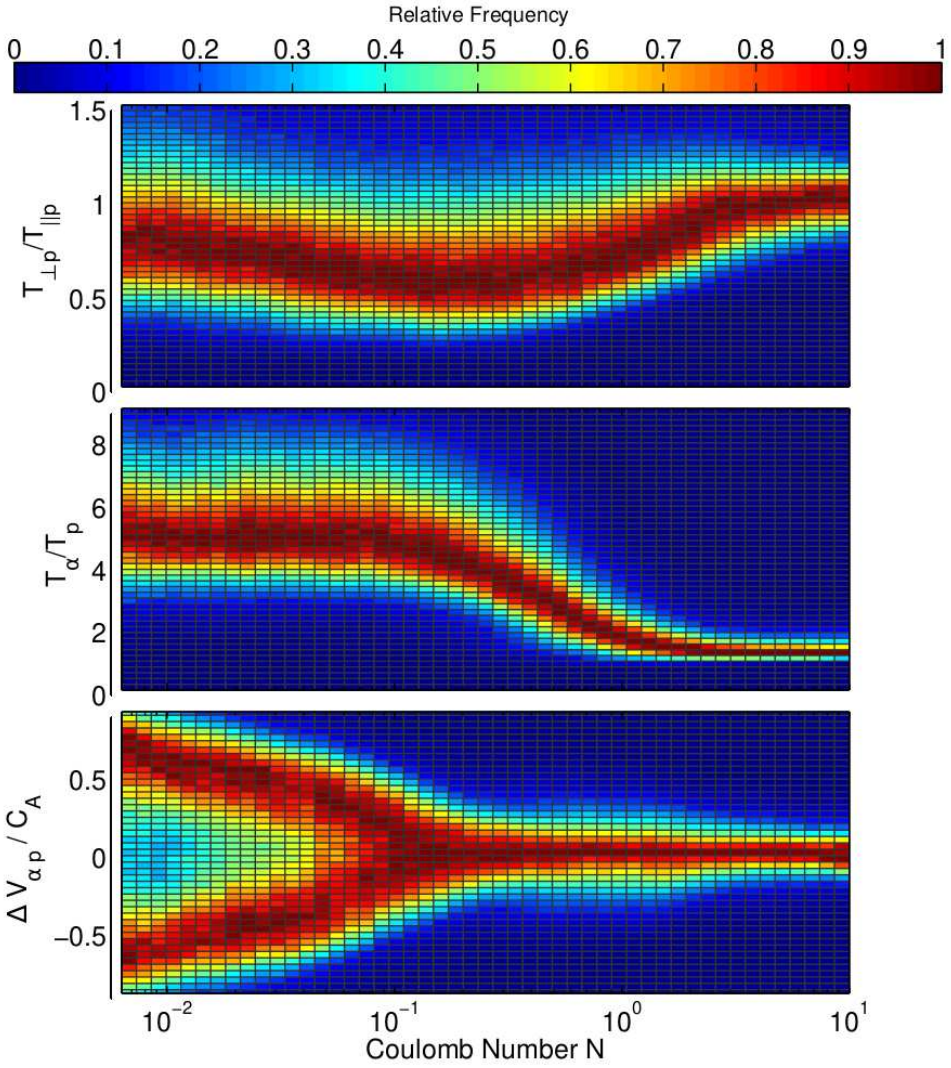

Kasper et al 2017 Wind

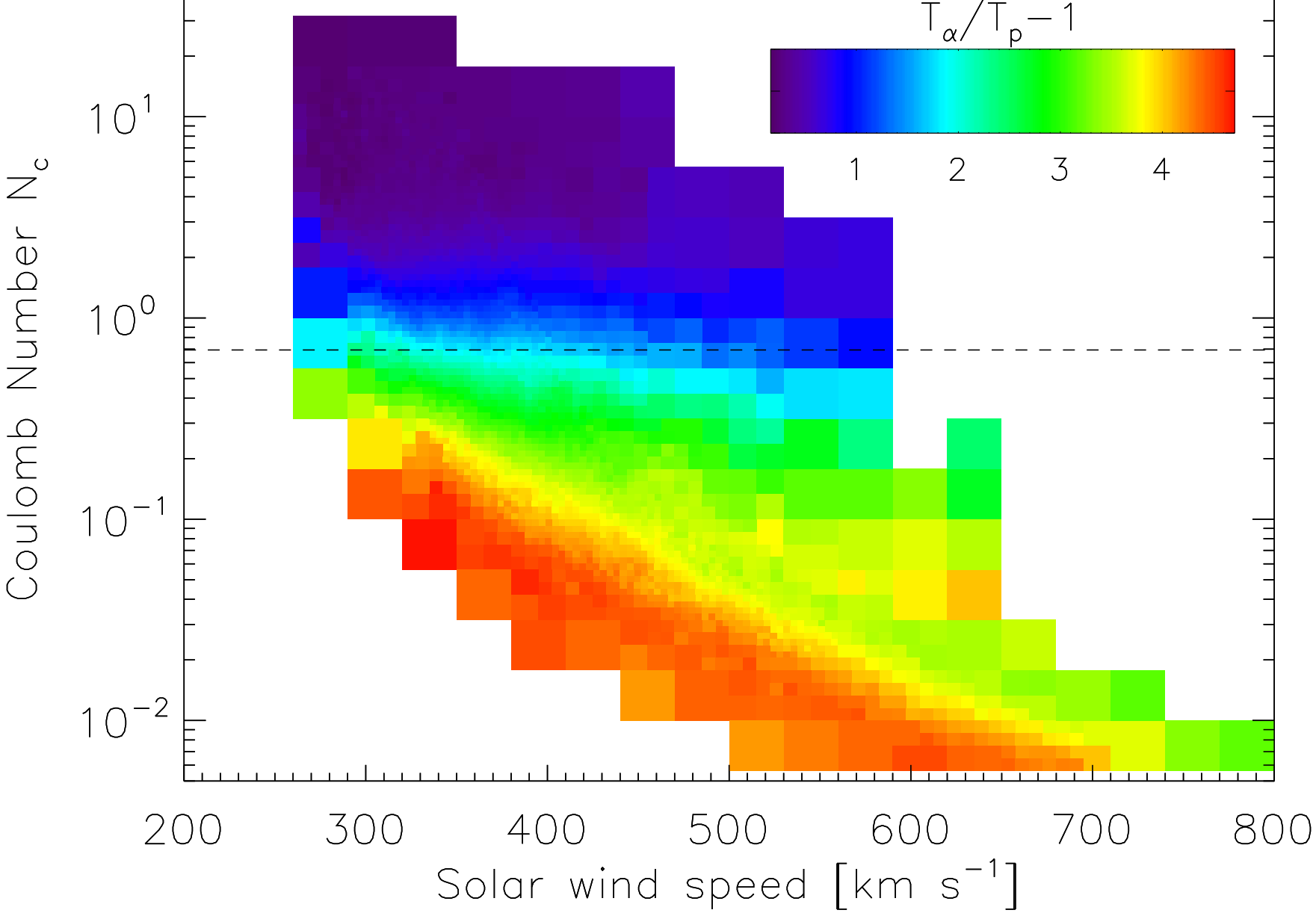

An exponential decay of $\epsilon \equiv T_\alpha/T_p - 1$ as a function of $N_c = \nu_{a,b}\frac{R}{V_{sw}}$ is seen for all V_{sw}. (Kasper et al 2017)

We assume all **preferential** heating of minor ions occurs within some zone, below a distance R_b from the Sun.

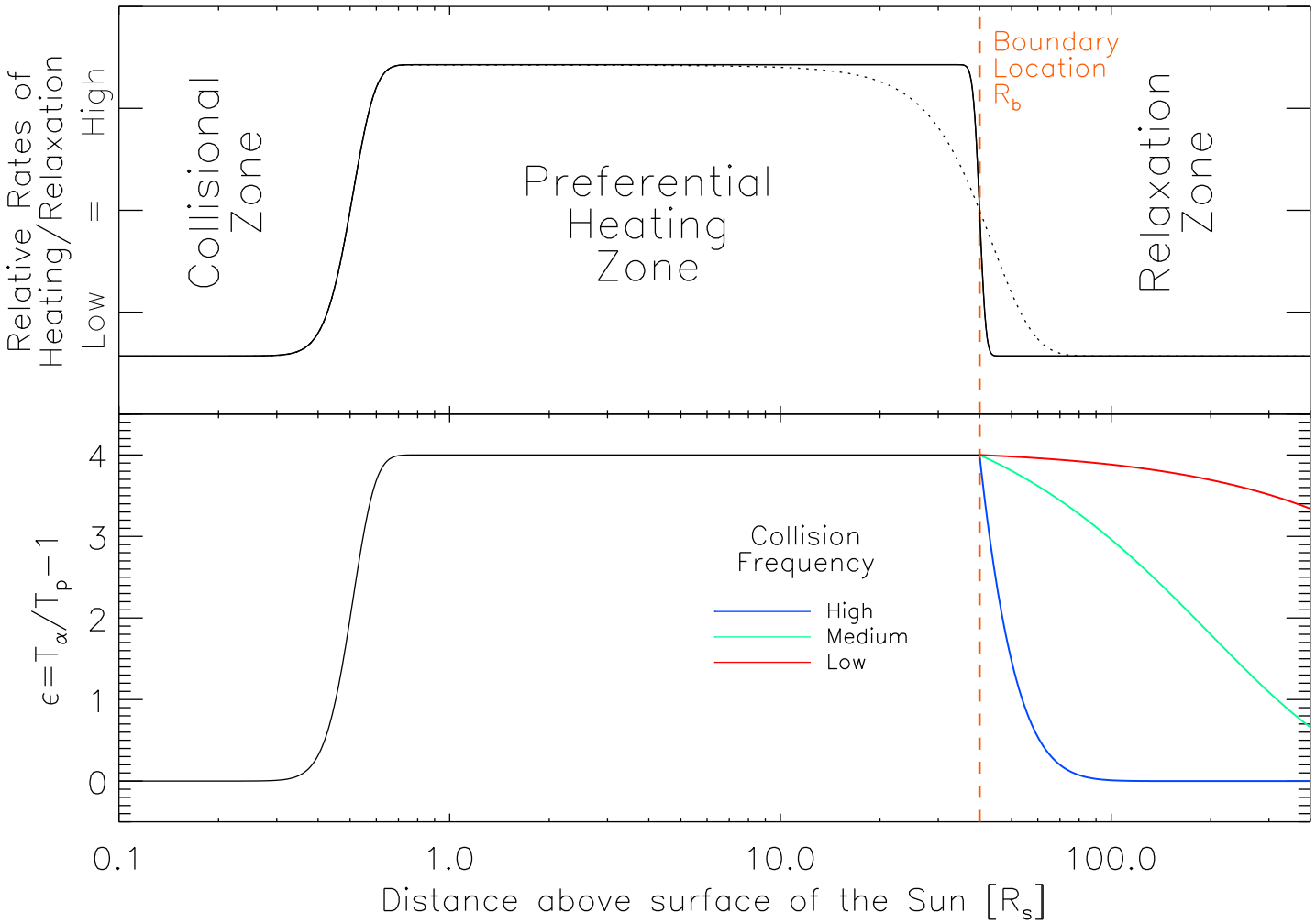

$\epsilon = T_\alpha/T_p - 1$ reaches an equilibrium value within the zone, and then relaxes as the solar wind expands.

Describing the Excess Temperature $\epsilon \equiv T_\alpha/T_p - 1$

We model the radial evolution of T_p and T_α as

$$\frac{dT_s}{dr} = (\gamma - 1)\left[\frac{T_s}{n_s}\frac{dn_s}{dr} - \frac{Q_s}{n_s k_B U}\right] - \sum_{s'} \frac{\nu_{ss'}}{U}(T_s - T_{s'})$$

If no **preferential** heating occurs beyond R_b (e.g. $Q_\alpha = Q_p \frac{n_\alpha T_\alpha}{n_p T_p}$ **or** $Q_s = 0$), we write

$$\frac{d\epsilon}{dr} = -\epsilon\left[\frac{\nu_{\alpha p}}{U} + \frac{\nu_{p\alpha}}{U}(\epsilon + 1)\right]$$

This results in a differential equation of the form:

$$\int_{R_b}^{R_w} \frac{2}{5}\frac{\left[1 + \frac{(\epsilon+1)}{4}\right]^{3/2} d\epsilon}{\epsilon(1+F) + \epsilon^2 F} = -\int_{R_b}^{R_w} \frac{\tilde{\nu}_{\alpha p}(r)}{U(r)} dr \equiv -A_c$$

The right-hand side is simply a sophisticated collisional age:

$$-\int_{R_b}^{R_w} \frac{\tilde{\nu}_{\alpha p}(r)}{U(r)} dr \equiv -A_c$$

with $\frac{\nu_{p\alpha}}{\nu_{\alpha p}} = \frac{n_\alpha m_\alpha}{n_p m_p} \equiv F$,

$\nu_{ss'} = 4\pi q_s^2 q_{s'}^2 \frac{\ln\Lambda n_{s'}}{m_s \mu w_{ss'}^3}$ (Hernandez & Marsch 1987) and

$$\tilde{\nu}_{ss'} = 8\pi q_s^2 q_{s'}^2 \frac{\ln\Lambda n_{s'}}{m_s^2 w_{s'}^3} = \frac{2\nu_{ss'}}{1 + m_s/m_{s'}} \left(1 + \frac{T_s m_{s'}}{T_{s'} m_s}\right)^{3/2}$$

The left-hand side 'simplifies' to:

$$\int_{R_b}^{R_w} \frac{2}{5} \frac{\left[1 + \frac{(\epsilon+1)}{4}\right]^{3/2} d\epsilon}{\epsilon\,(1+F) + \epsilon^2 F} = \frac{1}{10} \frac{\sqrt{5+\epsilon_w} - \sqrt{5+\epsilon_0}}{F}$$

$$- \frac{\sqrt{5}}{2\,(1+F)} \left[\frac{1}{2}\ln\left(\frac{\sqrt{1+\frac{\epsilon_w}{5}}+1}{\sqrt{1+\frac{\epsilon_w}{5}}-1}\right) - \frac{1}{2}\ln\left(\frac{\sqrt{1+\frac{\epsilon_0}{5}}+1}{\sqrt{1+\frac{\epsilon_0}{5}}-1}\right)\right]$$

$$+ \frac{(4F-1)^{3/2}}{10F^{3/2}\,(1+F)} \left[\tanh^{-1}\left(\frac{\sqrt{F}\sqrt{5+\epsilon_w}}{\sqrt{4F-1}}\right) - \tanh^{-1}\left(\frac{\sqrt{F}\sqrt{5+\epsilon_0}}{\sqrt{4F-1}}\right)\right]$$

Example Fits to Wind Data

For 25 km s^{-1} solar wind speed bins and fixed solar wind temperature and density radial trends, we fit

1) ϵ in the zone ϵ_0
2) residual ϵ when fully relaxed, ϵ_w, and
3) R_b

using Wind observations organized by Coulomb Age A_c

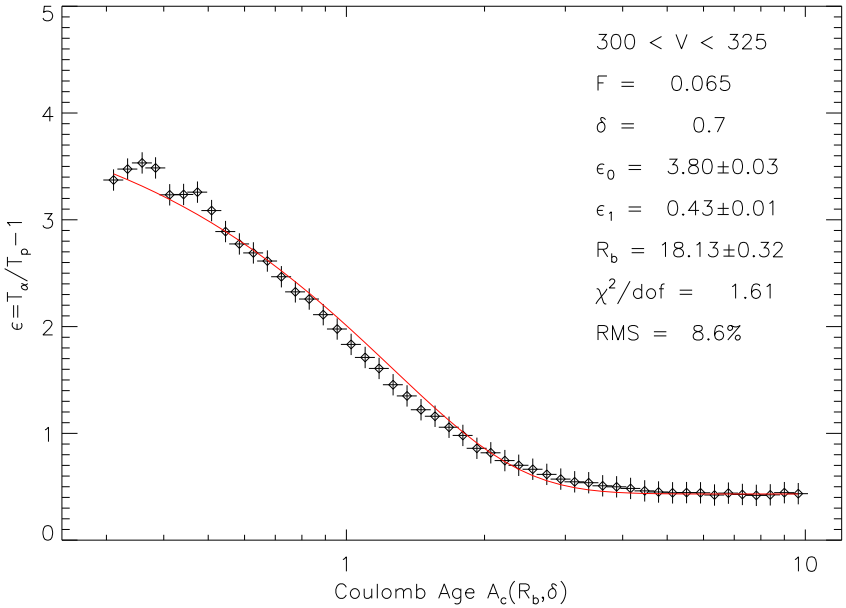

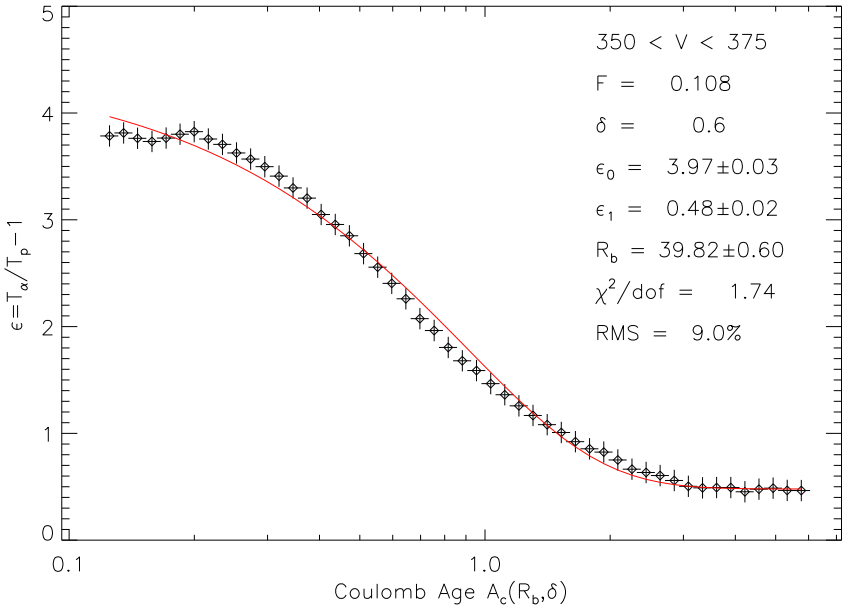

- Our model predicts ϵ to within $\sim 8\%$ of observational values with χ^2/dof~ 1.7.

Is there an Equilibrium ϵ in the Zone?

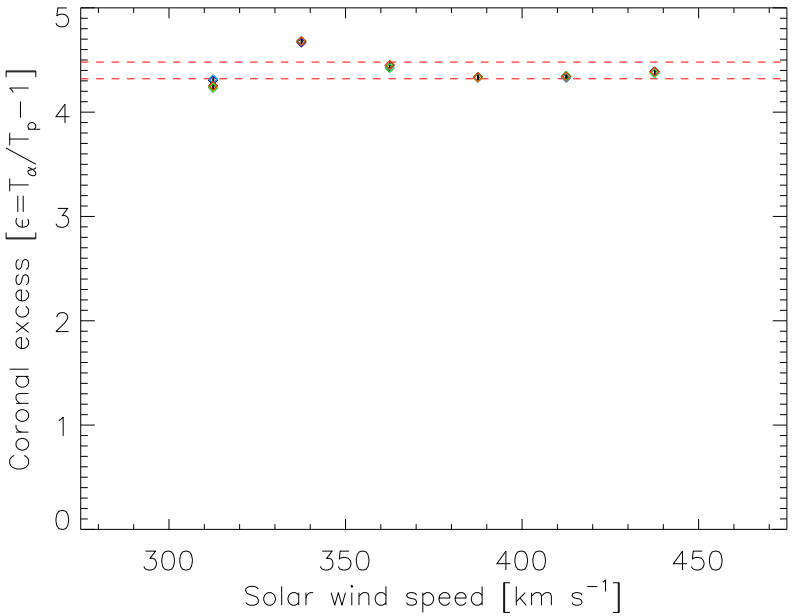

Kasper et al 2017 Wind

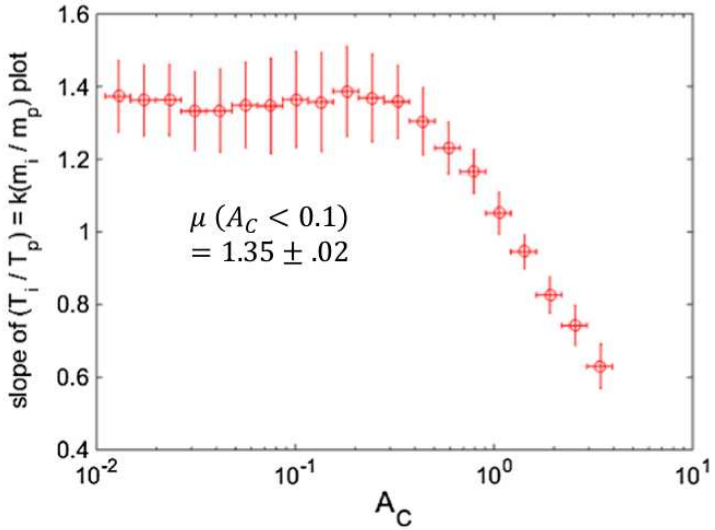

Tracy et al 2016 ACE

Regardless of wind speed and radial temperature trends, the excess temperature ratio $T_\alpha/T_p \approx 5.5$.

This agrees with heavier minor ion observations at 1 AU, which predict that collisionless minor ions should have $T_i/T_p = 1.35 m_i/m_p$.

What is the extent of this Zone?

Depending on V_{sw} and the radial profiles
$T_p \propto r^{-\delta}$ & $U \propto r^{-\sigma}$, $R_b \in [10, 55] R_\odot$.

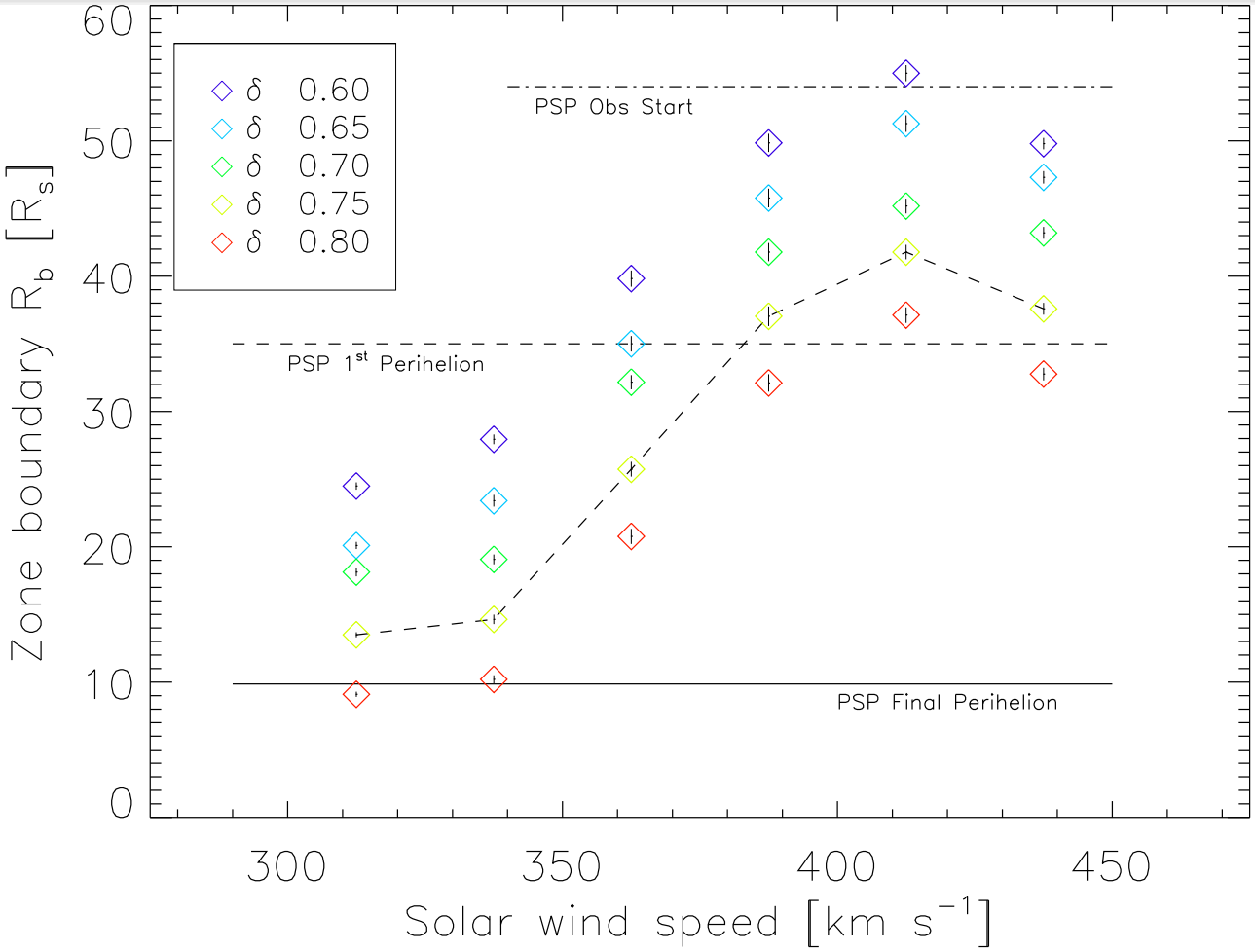

Kasper et al 2017

Does the Zone Move?

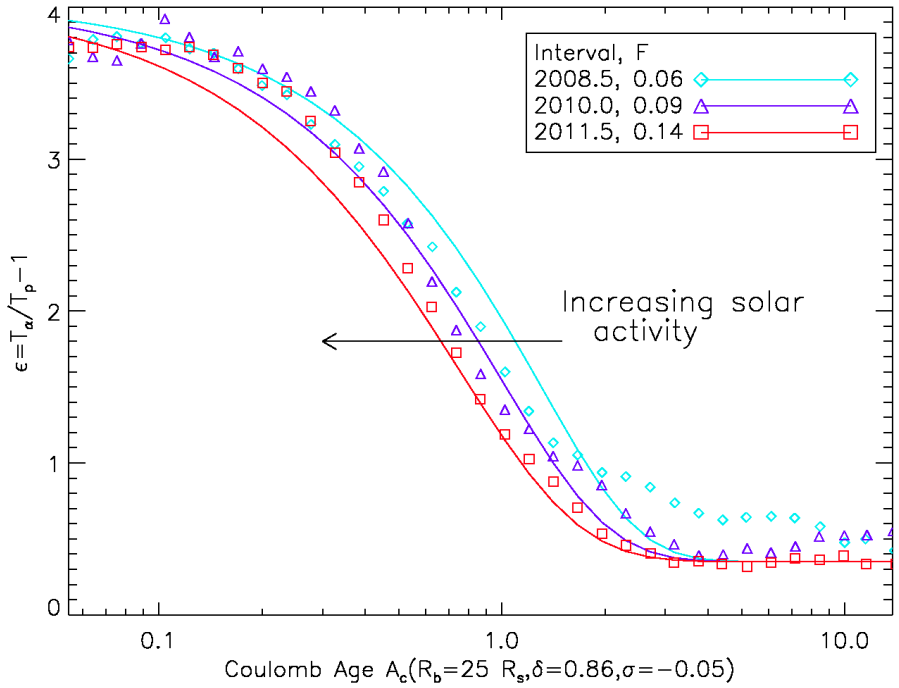

Calculating $\epsilon(A_c)$ for three 1.5 year intervals with fixed of $R_b = 25R_\odot$ hints that the zone moves in time.

At solar minimum, we overestimate R_b (ϵ decays too soon), but as activity increased it becomes an underestimate, suggesting R_b is moving outwards from the Sun.

Kasper & Klein, under review

Does the Zone Move? Yes.

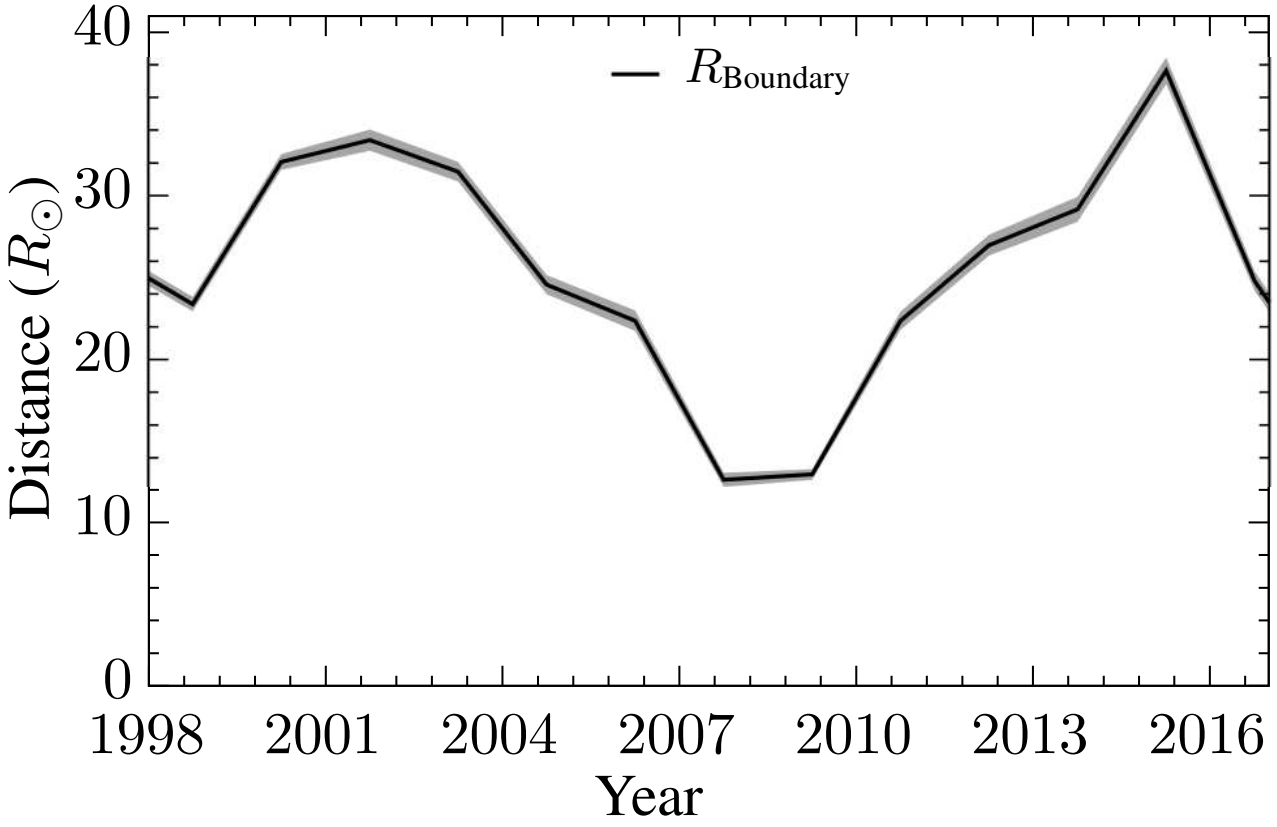

Kasper & Klein, under review

Using the same analysis, but dividing into 1.5 year intervals, we time dependent motion of R_b

Does the Zone Correspond to Solar Activity?

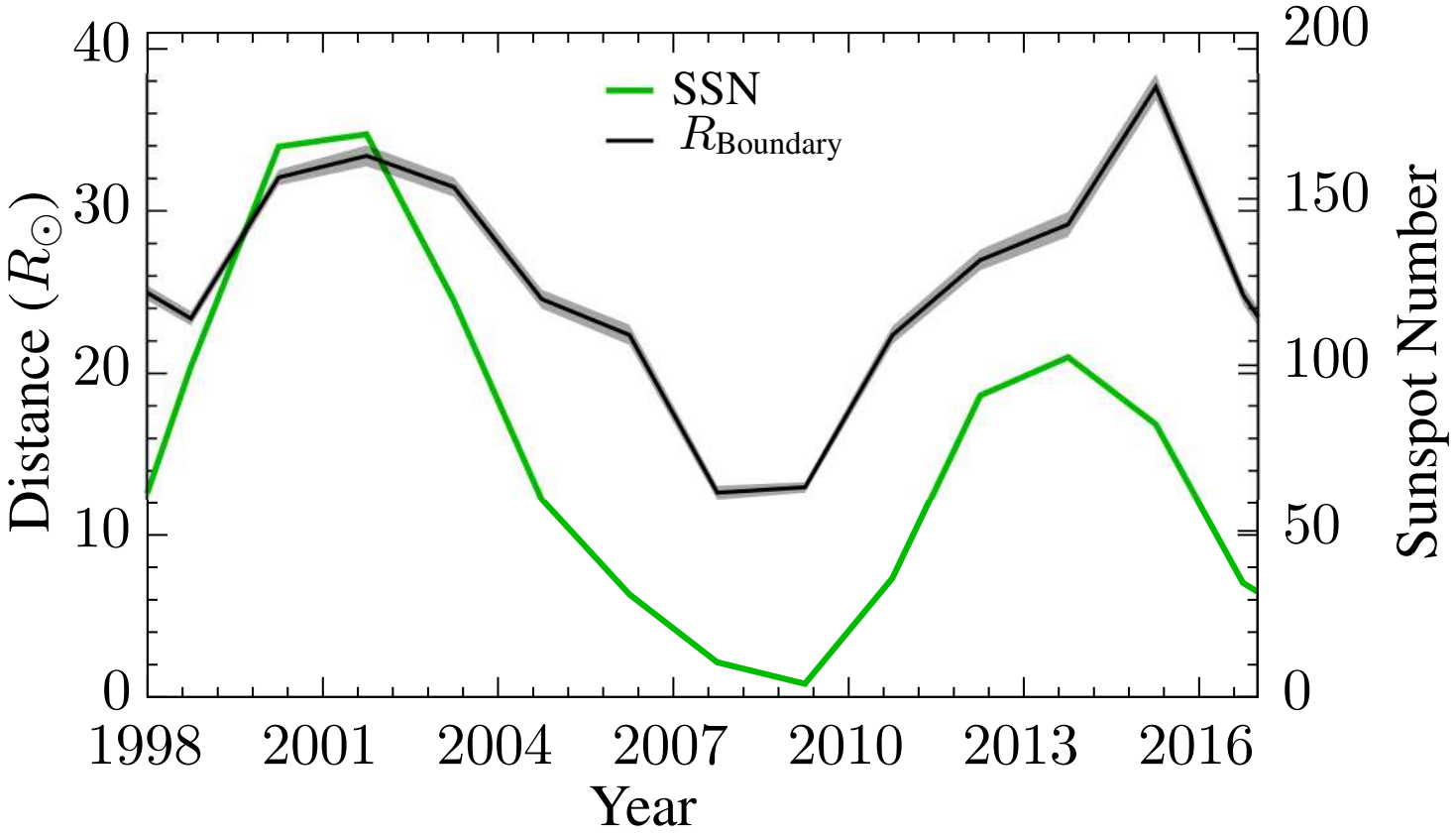

Kasper & Klein, under review

R_b is correlated with SSN ~ 0.84, indicating some connection to the solar cycle.

Does the Zone Correspond to a Characteristic Distance?

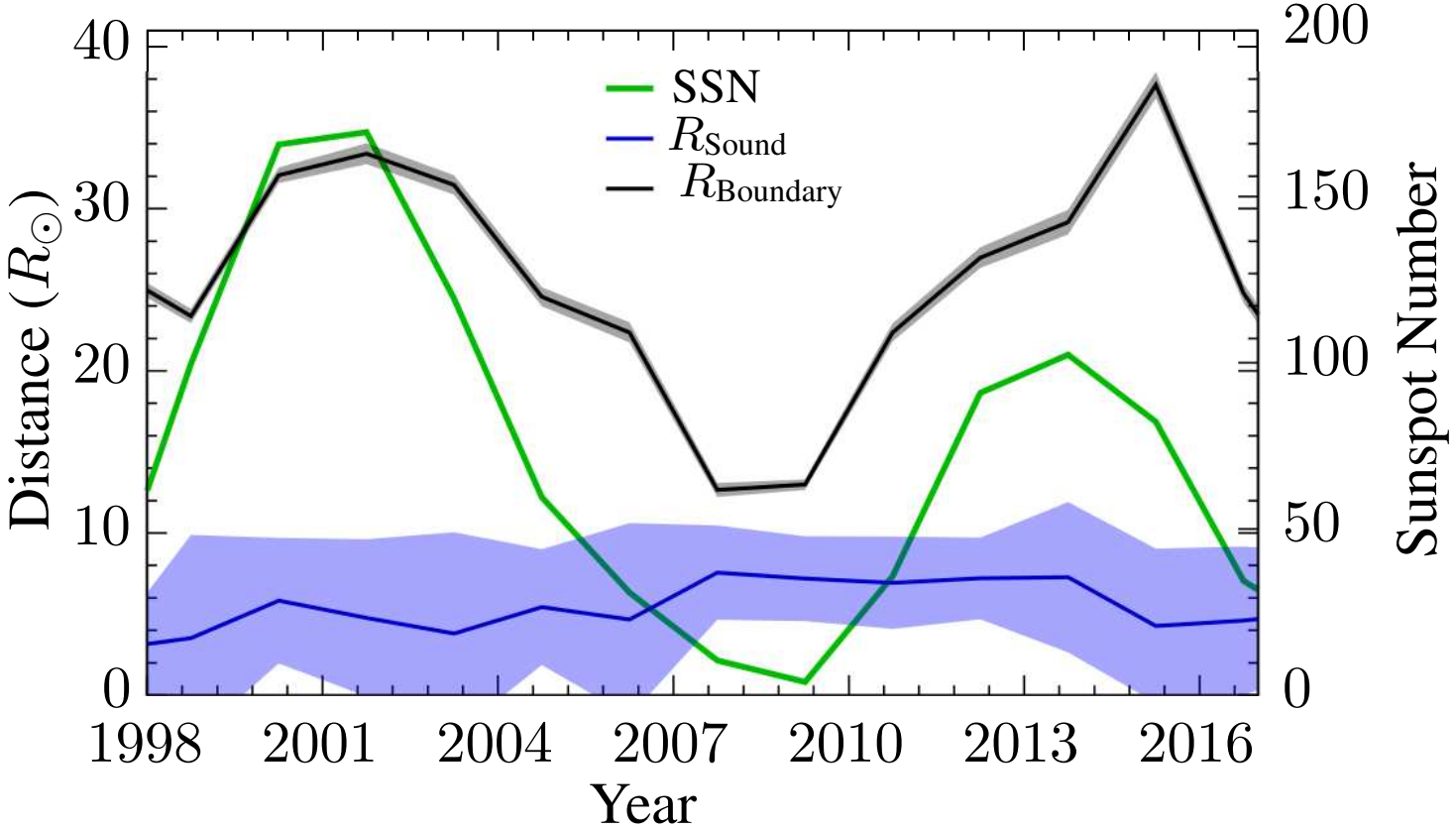

Kasper & Klein, under review

R_b is not well correlated with R_{sound} (~ -0.35).

Does the Zone Correspond to a Characteristic Distance?

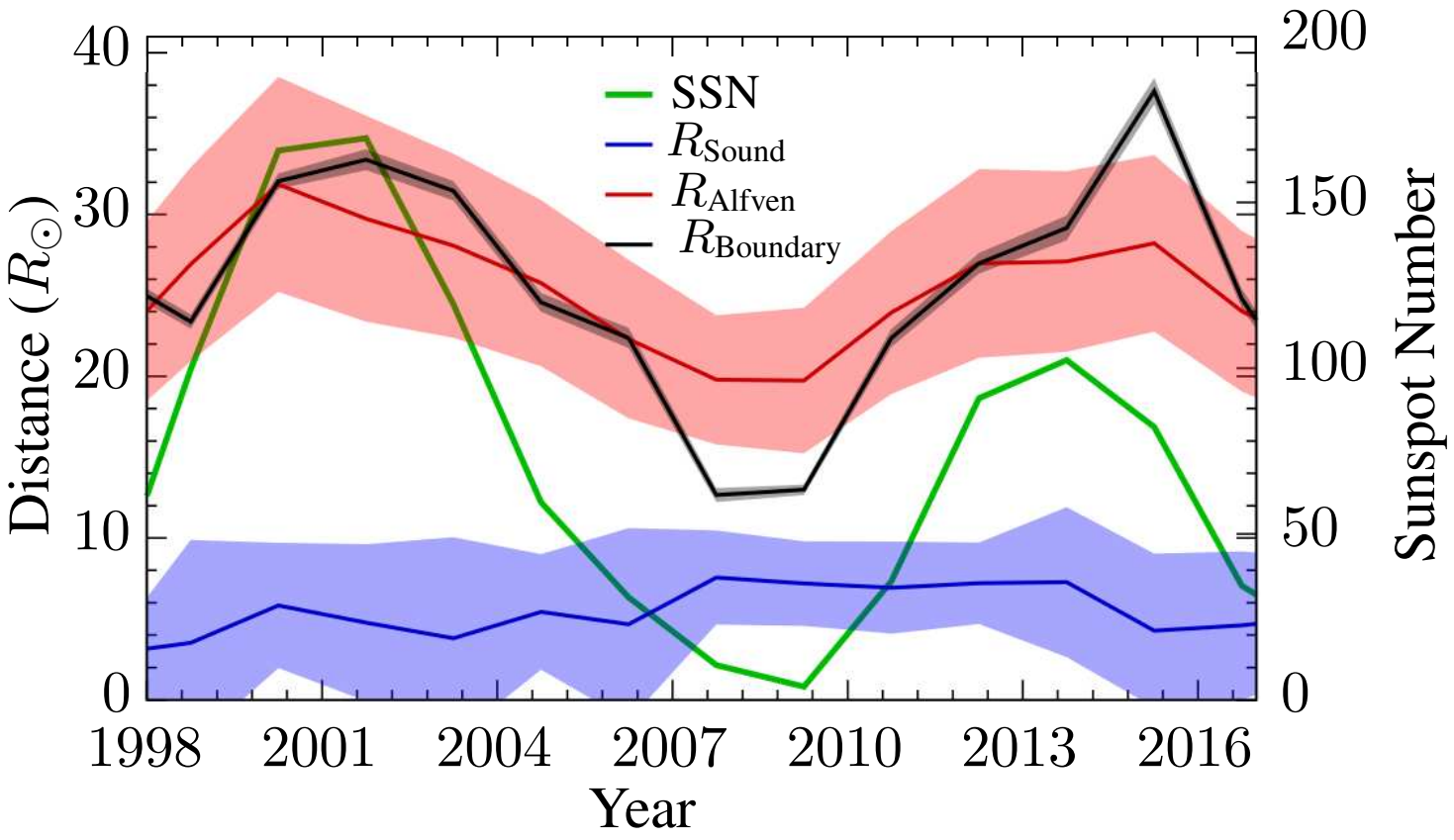

Kasper & Klein, under review

R_b is best correlated with the Alfvén surface (~ 0.95). This correlation holds regardless of the choice of radial exponents for U and T.

Parker Solar Probe: NASA's mission to 'touch the Sun'

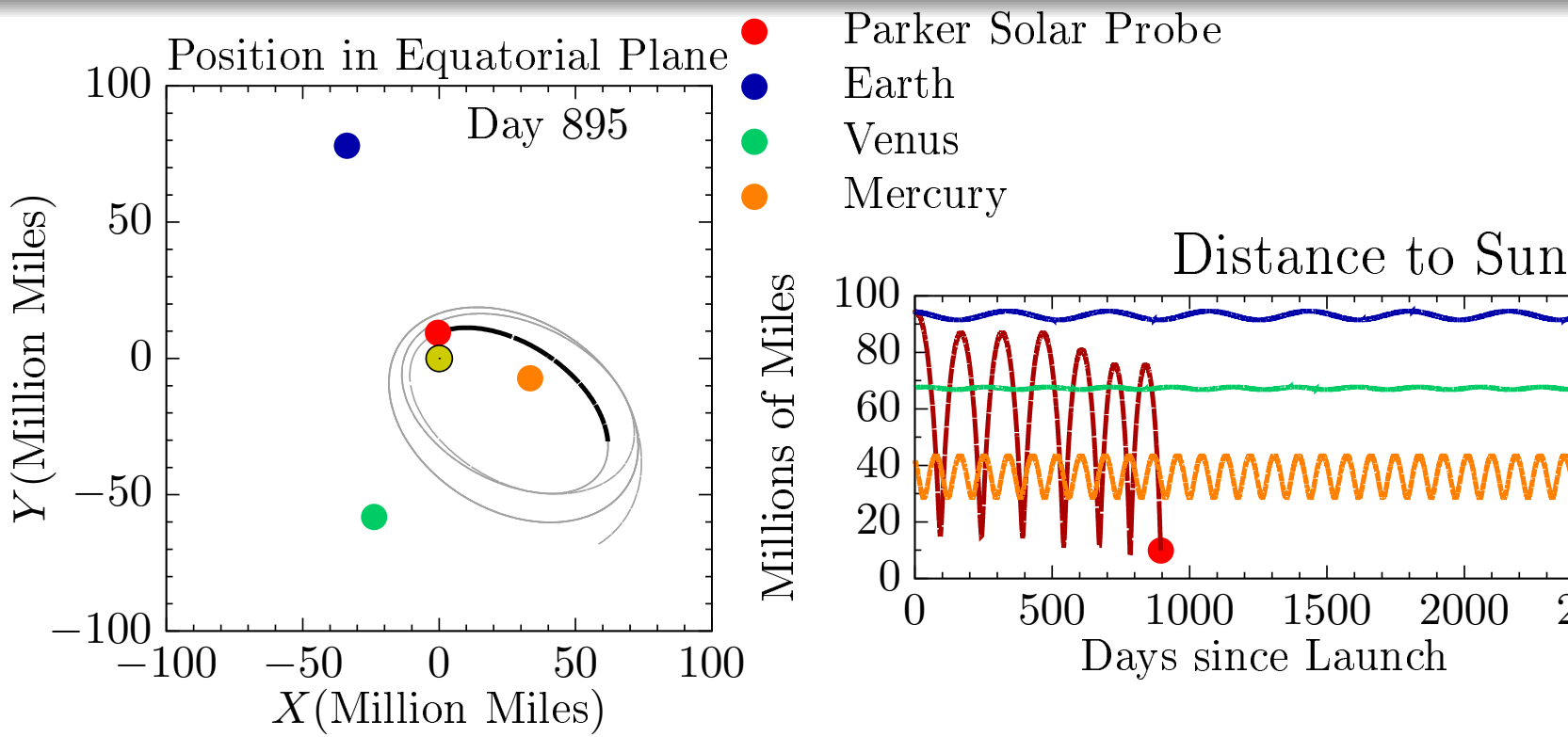

PSP will measure the local plasma (SWEAP) and E/M fields (FIELDS) at distances closer to the Sun than any previous mission.

One of the principle objectives is to "[t]race the flow of energy that heats the solar corona and accelerates the solar wind."

If interested in becoming familiar with SWEAP/Fields data formats, inquire about Working Groups.

When will we sample the preferential heating regime?

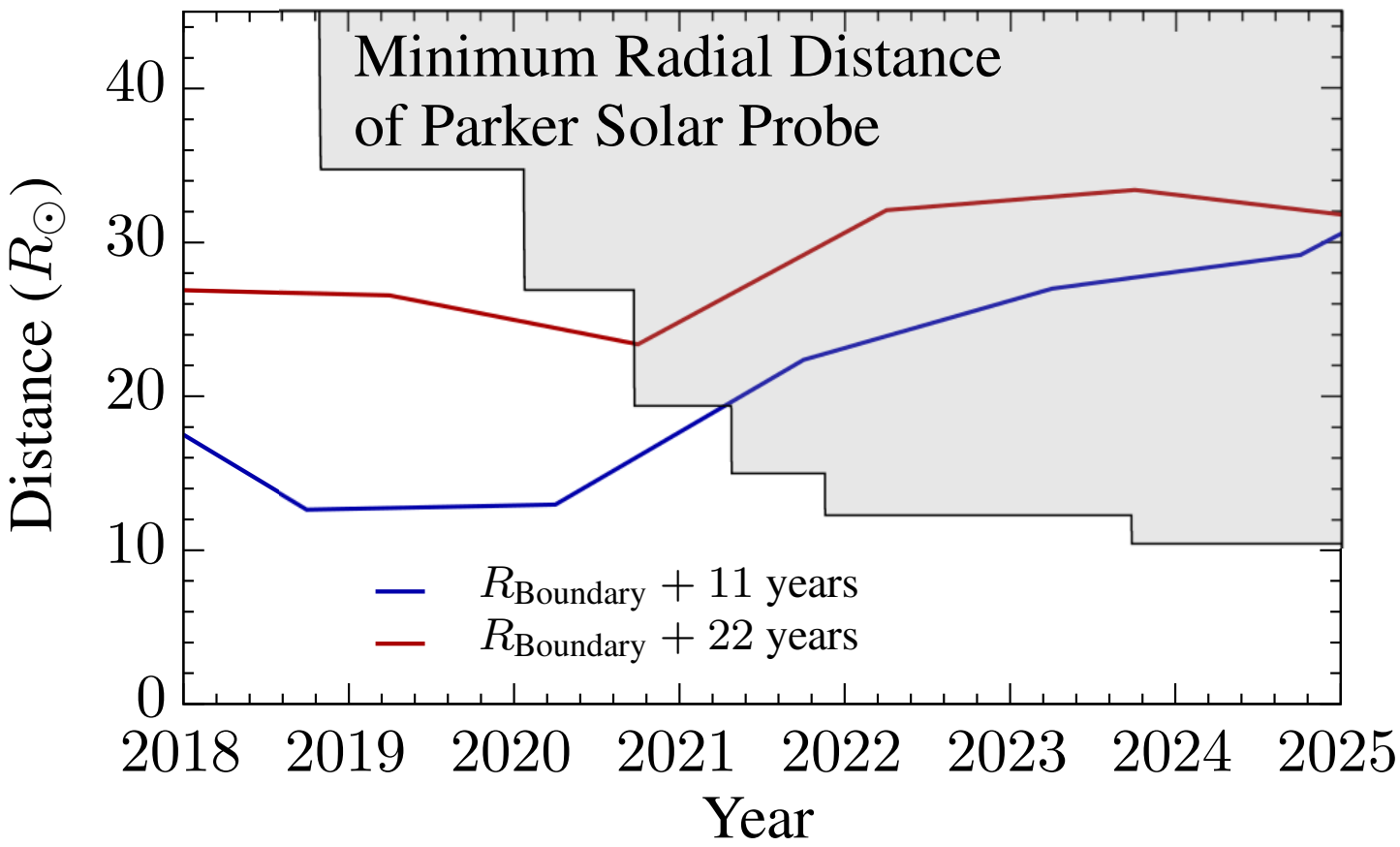

Kasper & Klein, under review

Based upon this model, we predict that the first in situ measurement of this preferential heating mechanism will be by PSP and will occur in 2020-2021.

In Conclusion

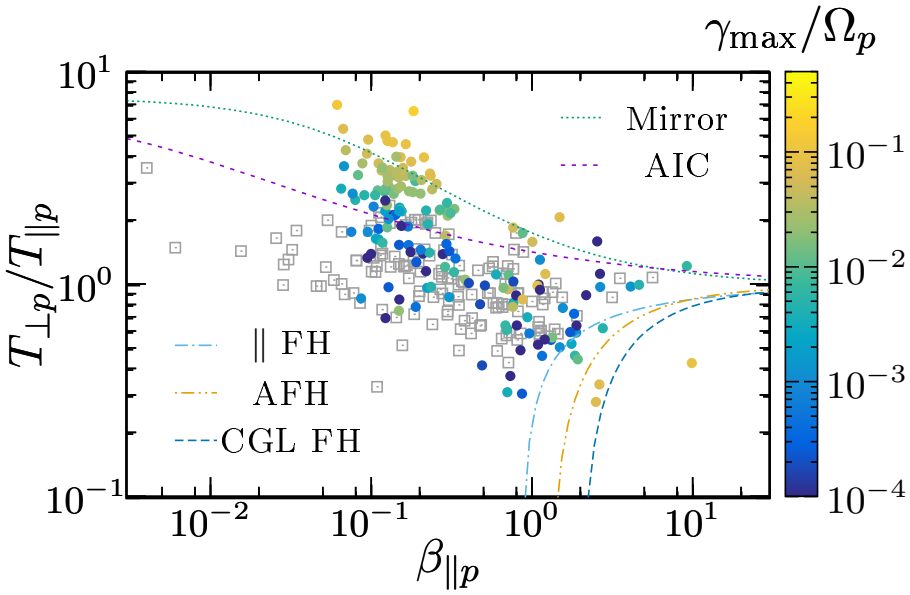

Klein et al 2018

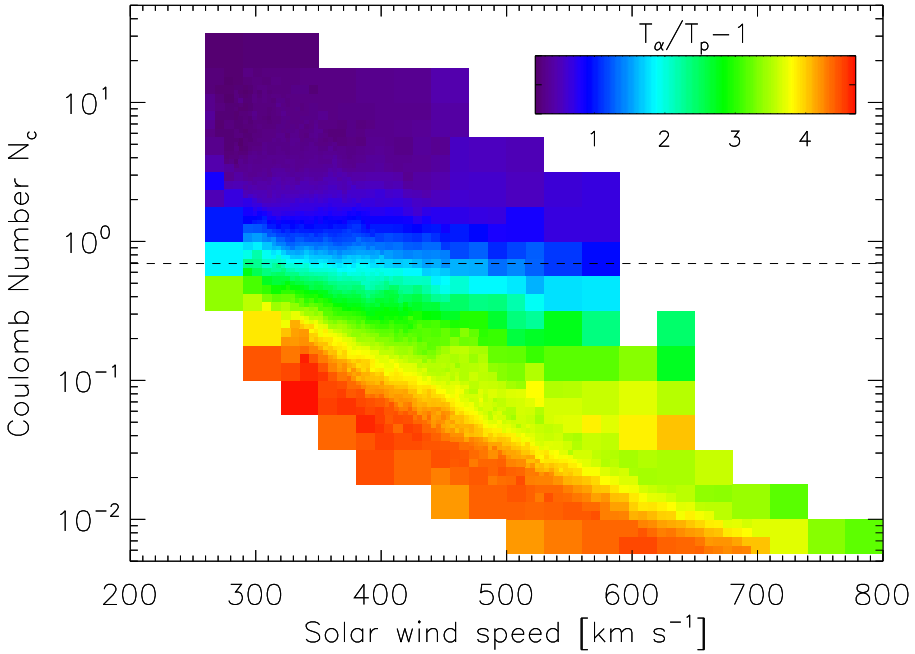

Kasper et al 2017

Non-thermal structure is ubiquitous and provides several sources of free energy to drive instabilities and limit macroscopic evolution.

Due to infrequent collisions, statistical studies of the nonthermal structure diagnoses distant processes, providing predictions for Parker Solar Probe and Solar Orbiter.

Future Concepts to Explore Space Plasma Processes

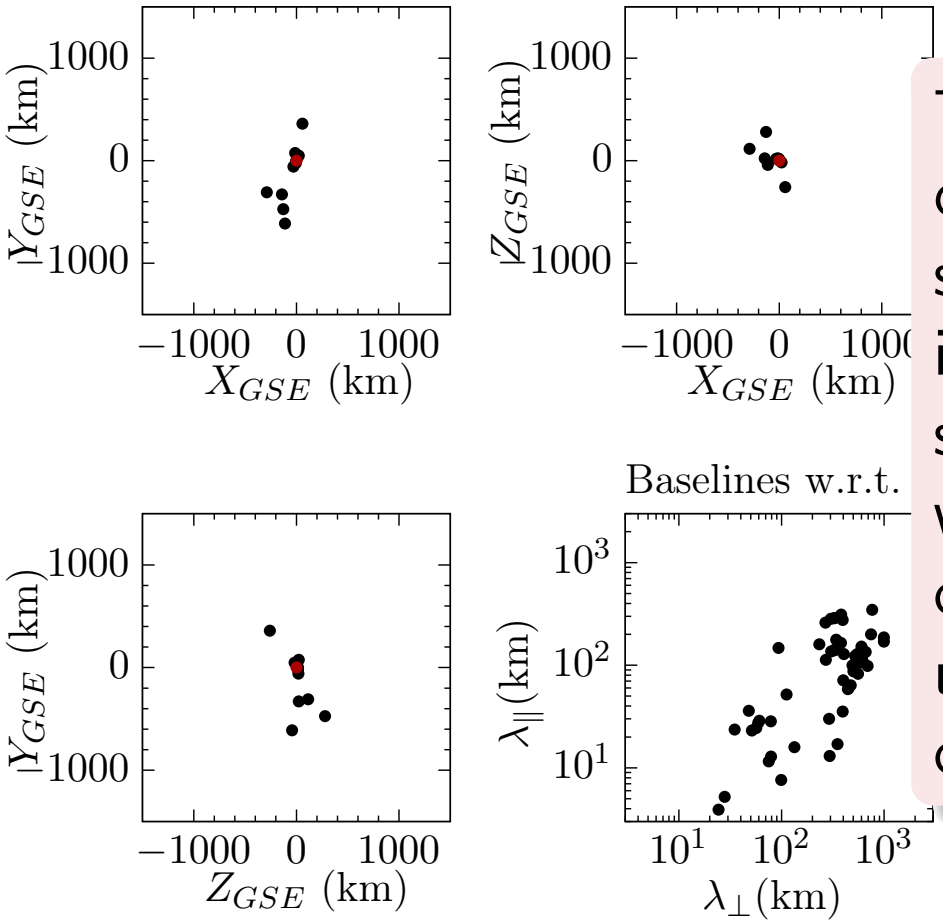

To-be-proposed missions comprised of many spacecraft, such as **HelioSwarm** with inter-spacecraft separations spanning large and small scales, will enable more detailed studies of energy transport, including unstable growth and its effect on the background turbulence.

Parametric Dependence of Ion-Driven Instabilities

$$\Delta X \equiv \frac{\bar{X}_{\text{unstable}} - \bar{X}_{\text{stable}}}{\bar{X}}.$$

	$\beta_{\parallel p}$	$10^4 v_{tp}/c$	$T_{\perp p}/T_{\parallel p}$	$T_{\perp \alpha}/T_{\parallel \alpha}$	$T_{\perp b}/T_{\parallel b}$
Total	0.60	1.07	1.57	0.96	1.48
Stable	0.50	0.91	1.12	1.03	1.39
Unstable	0.68	1.21	1.96	0.90	1.52
$\Delta X_{p,\alpha,b}(\%)$	19.12	13.46	50.59	-21.06	8.45
$\Delta X_{p,\alpha}(\%)$	132.53	57.59	-26.77	14.16	—

	$T_{\parallel \alpha}/T_{\parallel p}$	$T_{\parallel b}/T_{\parallel p}$	n_α/n_p	n_b/n_p	$\lvert v_\alpha\rvert/v_A$	$\lvert v_b\rvert/v_A$
Total	10.89	2.72	0.04	0.43	0.31	0.84
Stable	5.24	2.35	0.04	0.41	0.16	0.73
Unstable	15.74	2.88	0.05	0.44	0.44	0.89
$\Delta X_{p,\alpha,b}(\%)$	64.27	20.83	2.61	2.90	61.57	21.84
$\Delta X_{p,\alpha}(\%)$	26.46	—	18.10	—	77.44	—

No Global Minimum for Radial Trends